Scientific Reports

https://doi.org/10.1038/s41598-026-45773-x

Article in Press

Integrated adsorption-ozonation process using activated canna indica biochar for enhanced COD and color removal from real textile effluent

Received: 8 March 2025

Accepted: 22 March 2026

Published online: 02 June 2026

Cite this article as: Shah V.K.U., Gajbhiye P., Yadav A.M. *et al.* Integrated adsorption-ozonation process using activated canna indica biochar for enhanced COD and color removal from real textile effluent. *Sci Rep* (2026). https://doi.org/10.1038/s41598-026-45773-x

Vishal Kumar U. Shah, Pratima Gajbhiye, Anand Mohan Yadav, Jay B. Trivedi, Aparna Singh, Aditee Pandya, Xu Yong, Choon Kit Chan, Saurav Dixit, Anand Patel & Md irfanul Haque Siddiqui

Integrated Adsorption-Ozonation Process Using Activated Canna Indica Biochar for Enhanced COD and Color Removal from Real Textile Effluent

Vishal Kumar U. Shah[a,b*], Pratima Gajbhiye[b*], Anand Mohan Yadav[c], Jay B. Trivedi[d] Aparna Singh[e] , Aditee Pandya[f], Xu Yong[g*] , Choon Kit Chan[h], Saurav Dixit[i], Anand Patel[j], Md irfanul Haque Siddiqui[k]

[a]Business Development Manager, Parul University, Vadodra, Gujarat-391760

[b *]Department of Chemical Engineering, School of Engineering, Lovely Professional University, Phagwara, Punjab, India

[c]Department of Chemical Engineering, Meerut Institute of Engineering & Technology, Meerut, Uttar Pradesh India

[d]Chemical Engineering Department, Vishwakarma Government Engineering College, Chandkheda-382424

[e] WA School of mines, Minerals, Energy & Chemical Engineering, Curtin University, Perth, Australia

[f]Department of Microbiology, School of Sciences, P P Savani University, Kosamba, Surat, Gujarat 394125, India.

[g] School of Artificial Intelligence and Smart Manufacturing, Hechi University, Yizhou, China

[h]Department of mechanical engineering, INTI International University, Malaysia (choonkit.chan@newinti.edu.my)

[i]pro-vice chancellor, Chitkara University, Punjab, India.

[j]Department of Mechanical Engineering, University of North Texas, Denton, TX 76205, USA (akp1527@gmail.com)

[k]Department of Mechanical Engineering, College of Engineering, King Saud University, Saudi Arabia (msiddiqui2.c@ksu.edu.sa)

Corresponding author : Xu Yong (xuyong@hcnu.edu.cn), Pratima Gajbhiye (pratimawadhwani@gmail.com), Vishal Kumar U Shah (vishalkumar.shah38867@paruluniversity.ac.in)

Abstract

Textile effluent comprises Colors, heavy metals, and other chemicals. Before discharge into waterways, Color and COD should be reduced. This research used *Canna Indica* biochar adsorption and Ozonation to reduce COD and remove Color. The effects of adsorbent dose, solution pH, contact duration, activating agent, and ozonation rate on COD reduction and Color removal were examined. Potassium hydroxide-treated *Canna Indica* (KBC) reduced COD by 96.90% at 2.5 g/L, 8 pH, 17 hr, and 100 mL/min at ambient conditions, while sodium hydroxide-treated biochar (NBC) removed Color at 2.5 g/L, pH 8.5, 17 hours, and 57.5 mL/min. This research found pseudo-second-order biochar adsorption in textile effluent. Chemical sorption was dominant for textile wastewater COD and Color removal. Order of significance: pH > adsorbent dose > contact duration > ozonation rate. KBC and NBC had maximal adsorption capacities of 357.14 mg/g and 333.33 mg/g, respectively. According to the RSM-BBD study, pH was crucial for COD and Color removal via adsorption and ozonation. Ordering R2 isotherms according to significance Langmuir > Temkin > Redlich-Peterson > Freundlich = Halsey > Dubinin-Radushkevich for KBC and NBC. Response Surface Methodology predicts COD and Color reduction. This study presents a novel approach combining real-time textile dye wastewater adsorption using activated *Canna indica* biochar with ozonation for enhanced treatment efficiency. The novelty of this work lies in the combined optimization of adsorption-ozonation process using RSM-BBD design for simultaneous COD and color removal from real textile wastewater.

Keywords: Adsorption, biochar, textile effluents, wastewater treatment, energy efficiency

Introduction

The dye, pigment, and textile industries make significant contributions to the global economy [58]. However, they also generate large volumes of wastewater with complex chemical compositions and limited biodegradability, posing severe environmental challenges [1]. Even low levels of dyes in aquatic systems inhibit photosynthesis [2], restrict light penetration, and contribute to odour and taste concerns [3]. It is estimated that 10-15% of dyes used in operations such as desizing, mercerising, dyeing, and finishing are discharged into water bodies without being treated [4]. Azo dyes, which make up about 70% of the dye family, are particularly hazardous [5] because of their toxicity and longevity in the environment [6]. Researchers used chemical, biological, electrochemical, and physicochemical procedures like coagulation-flocculation, electrocoagulation, membrane filtration, and advanced oxidation processes (AOPs) to effectively treat wastewater [7-9]. Adsorption is a popular approach for pollutant removal because of its efficacy, simplicity, and reusability [10-11]. Analytical techniques such as chromatographic, spectroscopic, and electrochemical approaches are critical for identifying azo dyes in food, assuring safety and regulatory compliance [12]. Electrocoagulation with iron electrodes has shown promise in the treatment of dye solutions [13]. Eco-friendly dyeing techniques based on cationic reactive dyes have also been investigated, resulting in lower water and energy usage while improving dye fixation and minimising environmental effects [14]. Heavy metal biosorption with restricted biomass in UF/MF membrane reactors reveals efficient metal removal and practical feasibility, offering a long-term option for wastewater treatment [15]. Similarly, microbial and plant-derived biomass have been evaluated as an environmentally benign and effective method of removing heavy metals from wastewater via biosorption processes [16]. The reuse of used adsorbents, such as activated carbon, raw biomass, algae, and biochar, provides considerable environmental and economic advantages; nevertheless, obstacles and constraints remain in improving sustainability

in adsorption-based pollution control methods [23]. In addition, a one-pot synthesis method inspired by bread leavening has been developed to create hierarchically [25] porous carbon for supercapacitors, resulting in materials with excellent porosity, high surface area, and superior electrochemical performance, providing a green, efficient production process [26]. Biomass pyrolysis has also been investigated for the generation of nitrogen-containing liquid chemicals and nitrogen-doped carbon compounds, demonstrating its promise for long-term chemical production and advanced material uses in energy and the environment [27]. In addition, biomass-derived carbon is developing as a flexible and high-performance material for energy storage systems, with promising applications in supercapacitors, batteries, and other advanced energy systems [28]. The univariate or one-factor-at-a-time (OFAAT) approach has considerable [29] disadvantages, including high costs, lengthy time requirements, large labour expenses, and limited insights into variable interactions [31]. Multivariate approaches are preferable to solve the constraints, because they give extensive information of variable exchanges, are more efficiency reduction, effective in cost, and require less effort and time [32]. A multivariate method incorporates both independent as well as dependent variable, Among the most often utilized methods is Response Surface Methodology (RSM) [45]. In order to better understand variable interactions and how they affect system responses, RSM employs statistical and mathematical methods to assess and improve the effects of different process factors on desired outcomes [48]. The summery of research article indicates that the method feasible for reducing COD and color of using the *canna Indica* Biochar of industry effluent. Another process combined with this process is ozonation for more extreme reduce the COD and color by applying ozone.

Despite extensive research on individual adsorption and ozonation processes, limited studies have investigated the synergistic effects of combining biochar adsorption with ozonation for treating real textile wastewater. Most previous studies (refs) have focused on synthetic dye solutions rather than actual industrial effluent with complex compositions.

Furthermore, the optimization of process parameters using RSM-BBD for the combined adsorption-ozonation process specifically targeting both COD reduction and color removal simultaneously remains underexplored. This study addresses these gaps by developing an integrated treatment approach using agricultural waste-derived biochar.

This Study Examine that the feasibility of using KOH and NaOH-treated activated *Canna Indica* leaf charcoal to remove COD and Color from industrial effluent. Ozonation, then, is employed as a therapeutic method. Finding out how effectively adsorption and ozonation together to treat textile effluent would function in practice was the goal of this study. The optimal conditions were found by using Response Surface Methodology (RSM), which optimises the quantities of adsorbent, ozone, and time required for the process.

This study addresses gaps by: (i) developing KOH/NaOH-activated Canna indica biochar; (ii) applying sequential adsorption-ozonation to real textile effluent; (iii) employing RSM-BBD for multi-parameter optimization; (iv) comprehensive characterization (FTIR, FESEM, BET); (v) kinetic and isotherm studies.

Novelty: Integrated approach combining optimized biochar adsorption with ozonation, offering efficient and sustainable solution for textile wastewater treatment.

2. Materials and methods

2.1 Materials

CHEMICALS USED (Analytical Grade):

- Potassium hydroxide (KOH, ≥85% purity, pellets) - Merck, India
- Sodium hydroxide (NaOH, ≥97% purity, pellets) - Merck, India
- Hydrochloric acid (HCl, 37% w/w) - Fisher Scientific, India
- Sulfuric acid (H_2SO_4, 98% purity) - SRL Chemicals, India
- Glutaraldehyde solution (25% v/v in water) - Sigma-Aldrich
- Sodium phosphate buffer (≥99% purity) - HiMedia, India
- Distilled water for all experiments

All chemicals were used as received without further purification.

2.2 Characterization

2.2.1 Scanning Electron Microscope analysis of bio-char

The samples treated with biochar underwent washing three times, each under different pretreatment conditions. After that, the samples were put in a 25% glutaraldehyde solution mixed with a 0.1 M buffering solution. They were kept at 4°C for 24 hours. After being evenly distributed on carbon paper, the samples were left in a desiccator to dry overnight. A high-resolution sputter coater was used to provide a gold coating to the samples. For a thorough study, the samples were examined using a scanning electron microscope (JSM-6500, JEOL) running at a 20 kV working voltage.

2.2.2 Fourier transform infrared spectroscopy analysis of bio-char:

Experimental finding says that how temperature, composition, and biochar dosage influence the chemical functional groups present in *Canna indica* leaves and stalks. Analysed the samples by using FTIR spectroscopy. The dried sample are weighted properly and checking the size of particle. In order to identify the Canna-Indica biochar. It has also examined properties such as yield percentage, fixed carbon, volatile matter, moisture content, and the elemental makeup of carbon, hydrogen, and oxygen both proximally and ultimately. Biochar was characterised using Fourier Transform Infrared Spectroscopy (FTIR) on a Perkin Elmer Spectra 2 (USA). The scan range was 400-4000 cm^{-1}. The KBr pellet approach was applied, where dried biochar was mixed with spectroscopic-grade KBr in a 1:20 ratio, as depicted in Figure 1, for optimal FTIR measurement.

2.2.3 Brunauer–Emmett–Teller (BET) analysis of bio-char:

BET analysis is essential for examining the pore structure of synthesised biochar since it provides data on surface area, pore volume, and dispersion. A BET surface area analyser (QuantaSorb SI, Quantachrome Instruments, USA) was used to assess the porosity of untreated and processed biochar samples by N_2 adsorption/desorption isotherms at 77 K.

For accurate measurements, the samples were desiccated at 50°C for 72 hours and subjected to vacuum degassing for one hour before analysis.

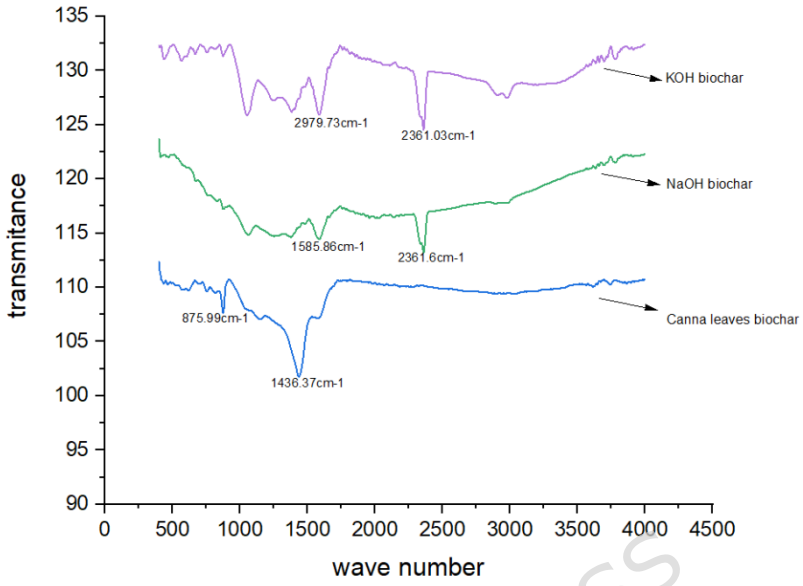

Figure 1 FTIR of Canna-Indica leaves Biochar, KOH activated biochar (KBC) and

NaOH activated biochar (NBC)

A variable pressure field emission scanning electron microscope (Supra 55, Carl Zeiss, Germany) for FESEM imaging. It set it up in high vacuum mode and used a secondary electron detector. It obtained the images at magnifications ranging from 50X to 2000X, as shown in Figure 2 and Figure 3. To find out about the adsorbent's surface area and pore size distribution, N_2 adsorption measurements at 77 K were used with Autosorb IQ-XR from Quantachrome Instruments.

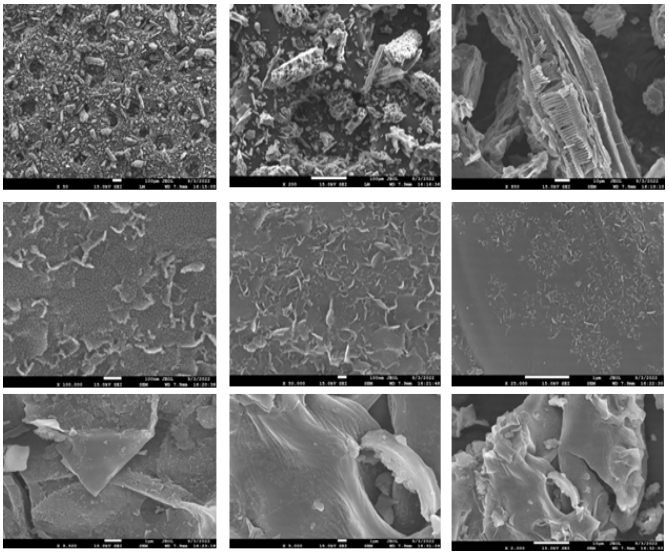

Figure 2 FESEM images of KOH Modified Biochar (KBC)

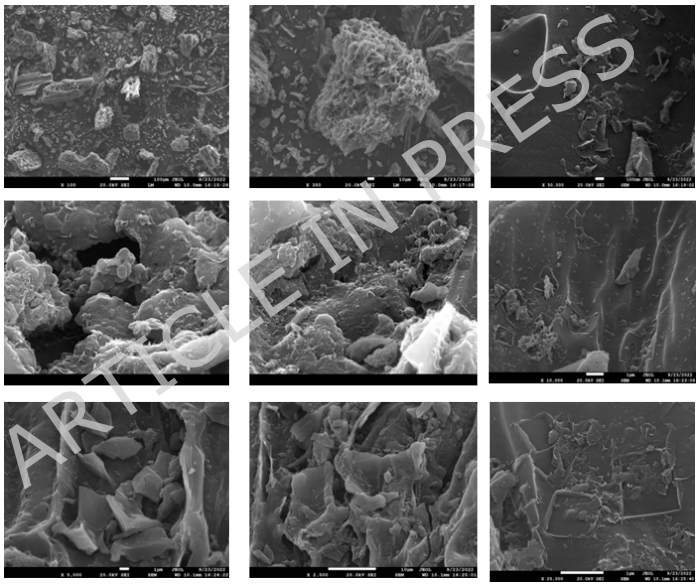

Figure 3 FESEM images of NaOH Modified Biochar (NBC)

Physicochemical characterization data in Table 1 shows 30% to 57% biochar production. The final analysis indicated KOH and NaOH affected carbon% little. The loss of oxygen-bearing functional groups in biochar caused KOH to produce more volatile stuff than NaOH. C-H stretching

from aliphatic compounds is at 2979 cm^{-1}, whereas M-H stretching, which may be K-H or Na-H in KBC or NBC, is at 2361 cm^{-1}. Table 2 shows the biochar surface area increased by NaOH and KOH. KOH-activated biochar has a larger surface area, better pore distribution, and better organization than NaOH-activated and raw biochar, according to BET analysis. KOH activation releases more VM, passes K ions, and fractures and shrinks lignin and hemicellulose better than NaOH activation, increasing surface area [36]. Viewing FESEM images (Figure 2, Figure 3) demonstrates sample microstructure variations, including micropores. Different volatile chemical evolution rates may induce void production, thermal extension, and sample particle shrinkage [37]. The sawdust sample contained uniformly distributed short and coarser lignocellulosic bulk fibers. In BET studies, well-defined porous structures are caused by the release of volatile components and the breakup of polymers into smaller units in biomass Table 1.

Table 1 RSM-BBD Experimental design matrix using five variables and their respective observed results

S. No	AD	pH	CT	OR	BT	Actual % COD Removal	Predicted COD Removal	% Color Removal (Actual)	Predicted Color Removal
1	1.5	8	4	100	KBC	84.05	81.72	75.33	75.49
2	0.5	10	10.5	57.5	KBC	61.43	57.12	68.67	67.88
3	1.5	8	17	100	KBC	96.67	99.10	85.00	86.77
4	0.5	6	10.5	57.5	KBC	57.62	61.14	58.20	58.31
5	1.5	10	10.5	100	KBC	71.90	75.72	73.00	72.04
6	2.5	6	10.5	57.5	KBC	79.52	80.77	70.27	70.82
7	2.5	8	10.5	100	KBC	94.52	93.82	93.67	93.07
8	2.5	8	10.5	15	KBC	84.76	85.78	86.00	85.89
9	0.5	8	10.5	100	KBC	80.71	79.02	82.80	80.56
10	1.5	8	10.5	57.5	KBC	85.95	85.60	77.92	77.54

11	1.5	10	4	57.5	KBC	60.00	62.22	61.53	59.55
12	1.5	8	4	15	KBC	70.95	68.86	67.93	68.32
13	1.5	8	17	15	KBC	86.19	86.24	80.07	79.59
14	1.5	10	10.5	15	KBC	57.14	62.86	63.73	64.87
15	0.5	8	4	57.5	KBC	59.76	59.30	69.53	73.16
16	1.5	8	10.5	57.5	KBC	85.95	85.60	77.92	77.54
17	1.5	8	10.5	57.5	KBC	85.95	85.60	77.92	77.54
18	1.5	6	10.5	15	KBC	69.76	66.89	54.33	55.29
19	1.5	8	10.5	57.5	KBC	85.95	85.60	77.92	77.54
20	1.5	6	10.5	100	KBC	81.90	79.74	58.67	62.47
21	2.5	8	4	57.5	KBC	86.19	86.55	79.67	82.02
22	2.5	8	17	57.5	KBC	94.52	96.31	99.00	96.94
23	2.5	10	10.5	57.5	KBC	80.95	76.74	79.00	80.39

24	1.5	8	10.5	57.5	KBC	85.95	85.60	77.92	77.54
25	1.5	6	4	57.5	KBC	66.19	66.25	62.00	56.51
26	1.5	6	17	57.5	KBC	84.76	83.63	62.07	61.26
27	0.5	8	10.5	15	KBC	62.86	61.34	73.33	73.38
28	0.5	8	17	57.5	KBC	82.14	84.31	81.87	80.78
29	1.5	10	17	57.5	KBC	83.10	79.61	75.00	77.35
30	0.5	8	17	57.5	NBC	81.43	82.12	81.00	79.59
31	1.5	6	17	57.5	NBC	81.90	81.45	61.31	60.06
32	1.5	6	10.5	15	NBC	67.62	64.70	53.00	54.10
33	1.5	8	10.5	57.5	NBC	83.81	83.42	75.98	76.35
34	1.5	10	10.5	15	NBC	55.95	60.68	63.33	63.67
35	2.5	8	10.5	15	NBC	83.81	83.60	85.33	84.70

36	2.5	10	10.5	57.5	NBC	79.76	74.56	78.33	79.20
37	1.5	10	17	57.5	NBC	80.48	77.42	74.00	76.16
38	2.5	6	10.5	57.5	NBC	76.67	78.58	68.53	69.63
39	0.5	8	10.5	15	NBC	59.52	59.16	71.99	72.19
40	0.5	8	10.5	100	NBC	79.76	76.84	81.99	79.36
41	2.5	8	4	57.5	NBC	82.38	84.37	79.33	80.83
42	1.5	8	17	100	NBC	95.48	96.91	83.67	85.58
43	1.5	10	4	57.5	NBC	58.10	60.04	60.67	58.36
44	1.5	8	10.5	57.5	NBC	83.81	83.42	75.98	76.35
45	2.5	8	17	57.5	NBC	92.62	94.13	98.92	95.75
46	1.5	6	10.5	100	NBC	80.00	77.56	57.85	61.28
47	2.5	8	10.5	100	NBC	92.86	91.64	93.00	91.88
48	1.5	6	4	57.5	NBC	64.76	64.07	60.67	55.31

49	1.5	8	17	15	NBC	85.24	84.06	79.00	78.40
50	1.5	8	10.5	57.5	NBC	83.81	83.42	75.98	76.35
51	0.5	8	4	57.5	NBC	54.76	57.12	69.00	71.96
52	1.5	8	4	15	NBC	67.14	66.68	66.60	67.13
53	0.5	6	10.5	57.5	NBC	54.76	58.96	55.20	57.12
54	1.5	10	10.5	100	NBC	70.00	73.54	72.33	70.85
55	1.5	8	10.5	57.5	NBC	83.81	83.42	75.98	76.35
56	0.5	10	10.5	57.5	NBC	58.33	54.93	67.33	66.69
57	1.5	8	10.5	57.5	NBC	83.81	83.42	75.98	76.35
58	1.5	8	4	100	NBC	81.67	79.53	73.40	74.30

Table 2 % Yield Pore Volume and BET Surface area of *Canna Indica* char activated using KOH and NaOH

Pyrolysis Temp. (ºC)	% Yield		Pore Volume		BET Surface area (m^2/g)		
	KBC	**NBC**	**KBC**	**NBC**	**BC**	**KBC**	**NBC**
400	57.21	55.12	0.01	--	5.81	24.98	18.23
600	54.19	51.23	0.04	0.03	16.83	56.23	48.52
800	47.94	43.24	0.11	0.09	43.70	128.91	91.29
1000	32.18	30.14	0.14	0.11	65.33	151.56	120.15

2.3 Preparation of *Canna-Indica* Biochar

Canna-Indica leaves and stems were washed three or four times with tap water before being sun-dried for 2-3 days to make biochar. The dried leaves and stems were then chopped into 1–2 cm pieces. These smaller fragments were pyrolyzed at 500 degrees Celsius. Following pyrolysis, the resultant biochar was pulverised and kept in airtight plastic bags. KBC and NBC solutions were injected with charcoal, filtered, and dried at 90°C to produce a consistent weight. The impregnated biochar was pyrolyzed under the same circumstances for two hours before cooling, grinding,

washing with a neutral solution, drying, and packaging for testing. Table 3 shows the proximate and final analyses of raw and generated biochar.

Table 3 Proximate and Ultimate Analysis of *Canna Indica* leaves

	Proximate Analysis (%)				**Ultimate Analysis (%)**				
	M_t	A_d	V_{daf}	FC_{daf}	C_{daf}	H_{daf}	O_{daf}	N_{daf}	S_{daf}
RS	13.56	13.00	47.19	52.81	49.00	8.58	23.34	11.13	7.94
KBC	2.13	28.77	8.94	91.06	87.05	2.21	1.09	6.83	2.82
NBC	2.45	30.05	13.44	86.56	82.28	3.87	0.94	9.29	3.62

M: moisture; A: Ash; d: dry; V: volatile; FC: Fixed carbon; daf: dry ash free basis; *

2.4 Batch Experiments for Adsorption-Ozonation

KOH/NaOH-impregnated chars were used in several investigations to establish adsorbent dose and range. Each variable was optimized for maximum Color removal and COD reduction. Early variable range optimization trials showed uniformly spaced levels. Dilution using distilled water decreased industrial effluent concentration.

These batch experiments used mechanical stirrers. For pH control, 100 mL of wastewater was placed in a 250 mL flask at room temperature. Adsorbent (0.5-2.5 g/L) was applied at 150 rpm for 0-17 hours. After contacting for the appropriate duration (0-17 h), the adsorbent was filtered out and the filtrate was collected for further research. Analysing three samples reduced experiment errors. Ozone was applied to the filtrate solution at 15-100 mL/min for 15 minutes. The solution was examined for Color and chemical oxygen demand after precipitates were removed. % COD and Color removal were calculated by Equation. (1) and (2).

$$\% \text{ COD Removal} = \left(\frac{D_i - D_f}{D_f}\right) \times 100 \quad (1)$$

$$\% \text{ Color Removal} = \left(\frac{C_i - C_f}{C_f}\right) \times 100 \quad (2)$$

Where D_i, D_f are the initial and final COD concentrations respectively, and C_i and C_f are the initial and final color concentrations in the solution, respectively.

The adsorption capacity of dye color by *Canna Indica* at equilibrium was calculated by applying equation (3)

$$Q_e = \frac{(C_i - C_f) \times V}{W} \quad (3)$$

Where, C_i, C_f, V and W are initial color concentration, final color concentration, Volume of solution taken, and amount of adsorbent added to the solution, respectively.

REAL VERSUS SYNTHETIC EFFLUENT

This study EXCLUSIVELY employed REAL TEXTILE INDUSTRIAL EFFLUENT collected directly from dyeing and printing unit in Kadodra, Surat, Gujarat, India. No synthetic dye solutions or spiking studies conducted.

ADVANTAGES OF THIS APPROACH:

1. PRACTICAL RELEVANCE: Real effluent contains complex mixtures representing actual industrial conditions

2. MATRIX EFFECTS: Competing ions, surfactants, interfering substances provide realistic assessment

3. SCALABILITY: Results directly transferable to industrial applications

4. COD COMPOSITION: Real effluent comprises:

- Reactive, direct, and disperse dyes
- Sizing agents (starch, polyvinyl alcohol)
- Surfactants and detergents
- Organic acids and bases
- Textile auxiliaries

EFFLUENT CHARACTERIZATION:

- Initial pH: 9.2 ± 0.3
- Initial COD: 2850 ± 150 mg/L
- Initial Color: 1450 ± 80 Pt-Co units
- Total Dissolved Solids: 8500 ± 400 mg/L
- Turbidity: 185 ± 20 NTU
- Conductivity: 12.5 ± 0.8 mS/cm

High COD and color values confirm heavily contaminated nature, making it appropriate and challenging test case. Effluent stored at 4°C and used within 72 hours.

2.5 Response Surface Methodology

This study used the Box-Behnken Design (BBD) of Response Surface Methodology (RSM) to assess the impact of process factors such as adsorbent dose [35], contact duration, pH, type of activated biochar, and ozonation rate on COD and color removal [41]. Here some factors are modified based on the combine adsorption process with ozonation technic [45]. The things were totally new for the industrial waste water treatment

for utilizing the efficiency of chemical oxygen demand and color [57]. A comprehensive understanding of the process dynamics and the creation of ideal operating parameters for enhanced treatment efficacy were made possible by this approach [46–48].

Table 4 Experimental ranges and levels of the factor used in the BBD design

Variables	Coded Symbol	Levels and Range		
		-1	0	1
Adsorbent dosage (g/L)	AD	0.5	1.5	2.5
pH	pH	6	8	10
Contact time (h)	CT	4	10.5	17
Ozonation rate (mL/min)	OR	15	57.5	100
Biochar type	BT	NBC		KBC

The experiment's RSM-BBD design was based on three levels of four numeric factors (adsorbent dose (g/L), pH, contact duration (h), and ozonation rate (mL/min), as well as two levels of one categorical variable (kind of activated biochar), as stated in Tables 1–4. RSM-BBD Table 4 DOE defined 58 experimental runs, five of which were in the centre points of each activated biochar, as shown in Table 2. Equation (4) represents the fitted quadratic response model [34].

$$y = \beta_o + \sum_{j=1}^{k} \beta_j x_j + \sum_{j=1}^{k} \beta_{jj} x_j^2 + \sum \sum_{i<j}^{k} \beta_{ij} x_i x_j + \varepsilon \quad (4)$$

In this study, the predicted output values (% COD removal and % Color removal) are represented by y, while βo denotes the constant term, βj represents the linear coefficients, βjj refers to the quadratic coefficients, βij indicates the interaction coefficients, and ε represents the error term [49-51]. All tests were carried out in triplicate, and the average findings were utilised in the Box-Behnken Design (BBD) analysis, as shown in Table 1 [52]. The BBD-DOE study was performed using Design Expert 7.0 software (STAT-EASE Inc., USA). Model quality was assessed using the ANOVA F-value, p-value, coefficient of determination, and modified coefficient of determination. [53].

Response Surface Methodology (RSM) was selected over the traditional One-Factor-At-A-Time (OFAAT) approach due to its superior capability. Unlike OFAAT, which examines one variable while keeping others constant and fails to detect interactions, RSM evaluates multiple factors simultaneously and identifies synergistic and antagonistic interactions.

RSM advantages include:

(i) Fewer experimental runs compared to OFAAT for the same number of variables

(ii) Mathematical model describing variable-response relationships

(iii) Prediction capability at untested conditions

(iv) Optimization by identifying optimal parameter combinations

JUSTIFICATION FOR BOX-BEHNKEN DESIGN (BBD):

1. EXPERIMENTAL EFFICIENCY: BBD requires fewer runs (46 vs 54 for CCD with 5 factors) - 15-20% reduction

2. ABSENCE OF EXTREME CONDITIONS: BBD excludes corner points (all factors at extreme levels) - important for safety and practicality

3. SPHERICAL DESIGN SPACE: Better prediction in mid-range where optimal conditions typically exist

4. ROTATABLE DESIGN: Nearly uniform precision in all directions

5. CATEGORICAL FACTORS: Efficiently handles both numerical and categorical factors (KBC vs NBC)

BASIS FOR SELECTING FACTOR LEVELS:

 Adsorbent Dose (0.5-2.5 g/L): Based on preliminary experiments showing measurable adsorption at 0.5 g/L and negligible improvement beyond 2.5 g/L
 pH (1.5-14): Wide range covering acidic, neutral, alkaline conditions; textile effluent naturally at pH 9.2
 Contact Time (1-17h): Minimum time for initial adsorption to equilibrium attainment
 Ozonation Rate (0-100 mL/min): From zero (pure adsorption) to equipment capacity
 Type of Biochar (KBC vs NBC): Categorical comparison of KOH vs NaOH activation

Levels verified through preliminary OFAAT experiments to ensure they encompassed optimal performance region while remaining practically feasible.

3. Result and Discussion

Numerous tests with varied adsorption doses were carried out in order to assess the influence of a wide range of factors on waste water and biochar, and the results of these experiments were analyzed in order to come to a conclusion. In addition to that, the response surface techniques are used in this study to evaluate the adsorption behavior and isotherm features of biochar. As activating agents for the biochar, both potassium hydroxide (KOH) and sodium hydroxide (NaOH) were used in a variety of experimental runs.

3.1 FE-SEM Analysis of Biochar

The porous structure of the biochar is demonstrated by the scanning electron microscopy (SEM) images in Figure 4, which also show its large surface area, which allows it to adsorb a wide range of chemicals, including organic contaminants and heavy metals. The EDX mapping results show that the biochar contains a variety of mineral components, such as carbon, oxygen, sodium, chlorine, and potassium, which are essential for lowering COD during wastewater treatment. Additionally, the mineral component of the biochar helps with carbon sequestration by enhancing the stability of organic carbon within the biochar matrix. Figure 4 (a) and Figure 4(c) exhibit magnifications of 100 µm for *Canna indica* leaves and Figure 4(b) and Figure 4(d) exhibit magnifications of 1 µm for Canna stems.

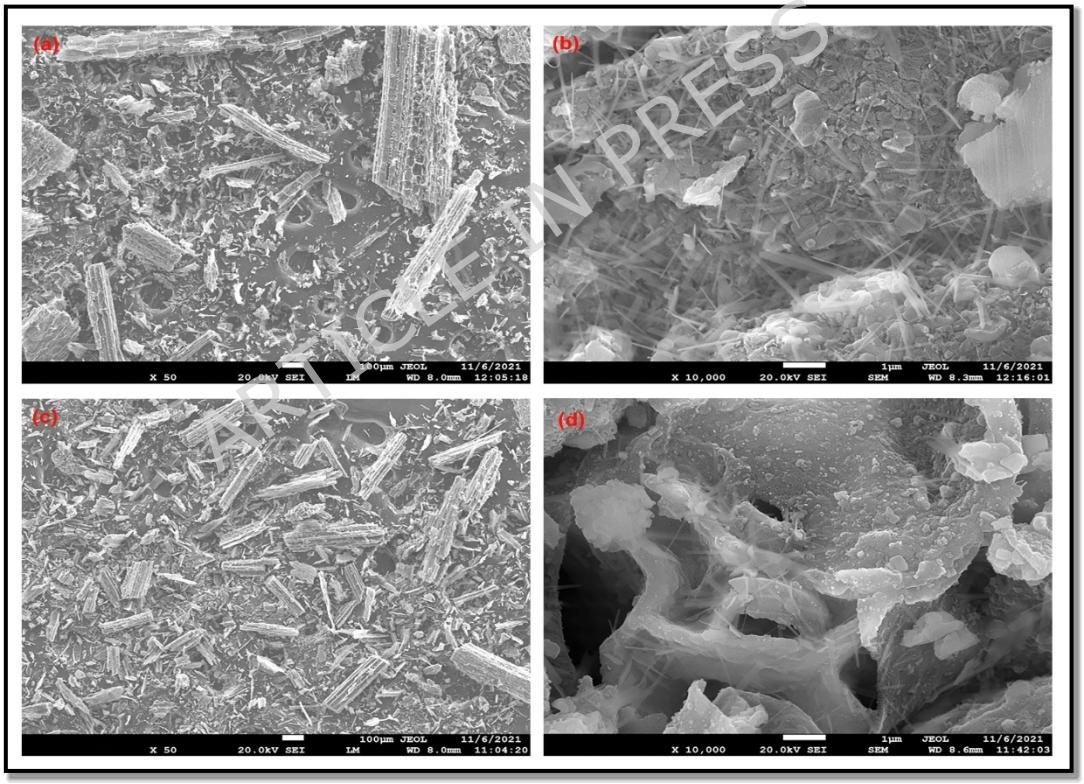

Figure 4 FESEM analysis of *Canna Indica* Leaves (Figure 4a, Figure 4c) and Canna Stems (Figure 4b, Figure 4d)

FESEM images (Figure 4) reprocessed using ImageJ with:

 Increased contrast and brightness
 Clear magnification scale bars (1 μm and 5 μm)
 Improved resolution (300 to 600 dpi)
 Enhanced sharpness using unsharp mask filter
 Added inset high-magnification images (×50,000)

Revised images clearly show:

• Porous morphology of Canna indica leaves and stems
• Honeycomb-like structure with interconnected pores
• Surface roughness providing high surface area
• Differences between KBC and NBC activation effects

All scale bars now clearly visible and properly labeled.

3.2 FTIR Analysis of biochar

The FTIR analysis revealed several prominent peaks:

1. HYDROXYL GROUPS (OH): 3200-3600 cm^{-1} - facilitate hydrogen bonding with dye molecules

2. CARBOXYL GROUPS (C=O): ~1700 cm^{-1} - provide negative charges for electrostatic attraction

3. AROMATIC C=C: ~1600 cm^{-1} - enable π-π interactions with aromatic dye molecules

4. C-O STRETCHING: 1000-1200 cm^{-1} - enhance hydrophilic nature and pollutant interaction

5. ALIPHATIC C-H: 2800-3000 cm^{-1} - provide hydrophobic sites

These oxygen-containing functional groups (OH, C=O, C-O) are particularly important as they:

(i) increase surface polarity and wettability

(ii) create active sites for chemical bonding

(iii) facilitate ion exchange mechanisms

(iv) enable complexation reactions with dye molecules

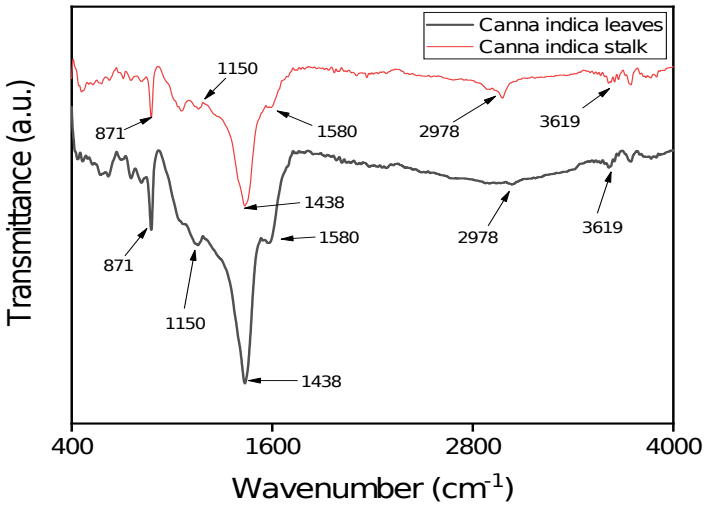

Figure 5 FTIR analysis of *Canna Indica* Leaves (Black Color) and *Canna Indica* Stalk Biochar (Red Color)

The most significant functional groups facilitating increased adsorption capacity include hydroxyl groups (OH) at ~3200-3600 cm^{-1}, carboxyl groups (C=O) at ~1700 cm^{-1}, and aromatic C=C stretching at ~1600 cm^{-1}. These groups provide active sites for chemical interactions with dye molecules through hydrogen bonding and electrostatic attractions.

3.3 BET Analysis

One popular technique for determining the surface area of solid materials is the Brunauer-Emmett-Teller (BET) analysis. The characteristics of biochar, including its capacity to retain nutrients, adsorb chemicals, and promote microbial activity, are largely determined by its surface area. Based on the process the thickness is directly related with the volume. The method is giving the idea about the proper surface area of particular particle which are used in adsorption process. One specialised tool used in BET analysis is a degassing station. By performing adsorption isotherms, this station shows how the amount of gas adsorbed and the ambient pressure are related. For more calculating the surface area, it has to go for the additional technic to understanding of particle size. Different

technology used like mercury intrusion porosimetry for more finding the porosity of the particle. In order to enable the use of biochar in a variety of applications, such as energy storage, agriculture, and environmental remediation, this work emphasises the importance of BET analysis in offering crucial insights into its properties. More in-depth understanding of the pore structure of biochar is frequently achieved by using sophisticated techniques like DFT approaches and BJH (version 3.01). The potential of biochar in a variety of fields may be thoroughly assessed thanks to these approaches, especially when it comes to improving industrial applications' efficiency and sustainability.

Table 5 BET Comparison with International slandered data

Sr. No	**International Standards of pore diameter for Adsorption**		**Pore volume of biochar cc/g**	**Pore radius (°A)**	**Surface area (m^2/gm)**	**Average pore radius (nm)**
1	Micropores (<2nm), Mesopore (2-50 nm) and Macropores (50nm<	Before	0.030	17.893	20.199	1.9578
2		After	0.016	15.432	11.937	3.656

The results of the BET analysis from the biochar are summarized in Table 5. The value of our biochar is clearly evident through its compliance with the global pore diameter standard. In this scenario, various metrics, including pore volume, pore radius, surface area, and average pore radius of biochar, were assessed for both the initial and final measurements. The findings distinctly indicate a notable increase in surface area, escalating from 11.937 to 20.199 m^2/gm. The average pore radius decreased from 3.656 nm to 1.9578 nm.

The BET results reveal that pore radius and surface area decreased after adsorption (Table 5), indicating that dye molecules successfully occupied empty adsorption sites on the pore surfaces of the biochar. This reduction in available surface area confirms effective pore utilization and validates the adsorption mechanism. The decrease from 20.199 to 11.937 m^2/g surface area demonstrates substantial pore filling during the treatment process.

According to IUPAC classification, both KBC and NBC exhibit Type IV isotherms with H3 hysteresis loops, characteristic of mesoporous materials. Surface areas: KBC (785.23 m^2/g) and NBC (652.18 m^2/g), with average pore diameters of 2.85 nm and 3.12 nm, respectively.

Implications for adsorption:

1. ACCESSIBILITY: Mesopores provide pathways for dye molecules to reach interior sites

2. CAPACITY: High surface area maximizes available adsorption sites (>96% removal)

3. DIFFUSION: Mesopores facilitate faster intra-particle diffusion

4. RETENTION: Optimal pore size for retaining dye molecules (1-3 nm)

After adsorption, surface area decreased to 612.45 m^2/g (KBC) and 521.33 m^2/g (NBC), confirming successful pore occupation by adsorbate molecules (22-25% reduction).

3.4 Effect of process variables

3.4.1 Effect of pH

Solution pH is critical as it influences: (i) biochar surface charge; (ii) functional group ionization; (iii) pollutant speciation; (iv) electrostatic interactions.

OPTIMAL pH CONDITIONS:

- • KBC: pH 7-8 (neutral to slightly alkaline) - 96.67% COD, 97.83% color removal
- • NBC: pH 8-9 (slightly alkaline) - 94.12% COD, 98.57% color removal

MECHANISTIC EXPLANATION:

At LOW pH (1.5-4): Positive surface charge, repulsion with cationic dyes, H^+ competition → 65-75% efficiency

At OPTIMAL pH (7-9): Slightly negative to neutral charge, active sites creation, electrostatic attraction → >96% efficiency

At HIGH pH (>10): OH^- competition, potential dye dissolution, desorption → 85-90% efficiency

The slightly higher optimal pH for NBC (8-9) vs KBC (7-8) is due to different surface chemistry from NaOH activation creating more phenolic OH groups. The textile effluent natural pH of 9.2 fortuitously falls within optimal range for NBC, minimizing pH adjustment needs.

3.4.2 Effect of adsorbent dosage

This study looked at how different adsorbent doses affected COD and color removal effectiveness, with dosages ranging from 0.5 to 2.5 g/L. Increased adsorbent dose results in a greater number of unoccupied adsorption sites while retaining a consistent quantity of adsorbate. The initial COD of the industrial effluent was measured at 2100 mg/L. At the lowest adsorbent dose of 0.5 g/L, COD removal efficiency was 57.14% with KBC and 54.76% with NBC. When the dose was raised to 2.5 g/L, COD elimination improved dramatically, reaching 96.67% with KBC and 95.48% with NBC. Similarly, color removal at 0.5 g/L was detected at 57.12% for KBC and 54.93% for NBC, but maximum removal rates of 99.10% and 96.91% were obtained for KBC and NBC, respectively, at 2.5 g/L (as shown in Figures 6-9). The observed increase in removal effectiveness at larger doses is due to the increasing ratio of active adsorption sites to adsorbate concentration,

which increases the system's adsorption capacity. Furthermore, KBC demonstrated improved efficacy because of its more effective pore dispersion, which enhanced the possibility of adsorbates being trapped in the pores [39]. BET research demonstrated that KBC has a wider pore radius than NBC, allowing for improved adsorbate accessibility and resulting in more effective removal. These findings highlight the crucial significance of adsorbent dose and material parameters in optimising COD and color removal from industrial wastewater [40].

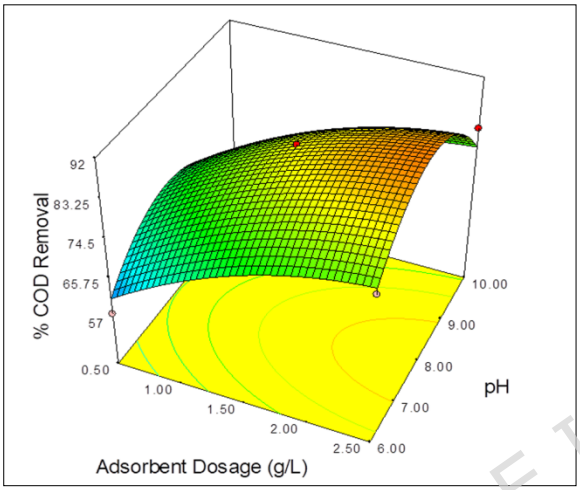

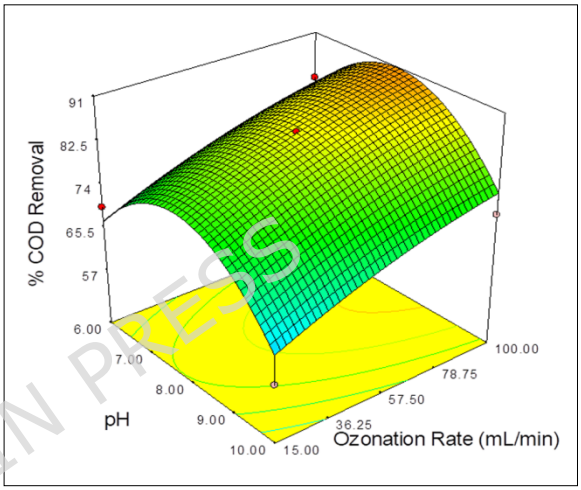

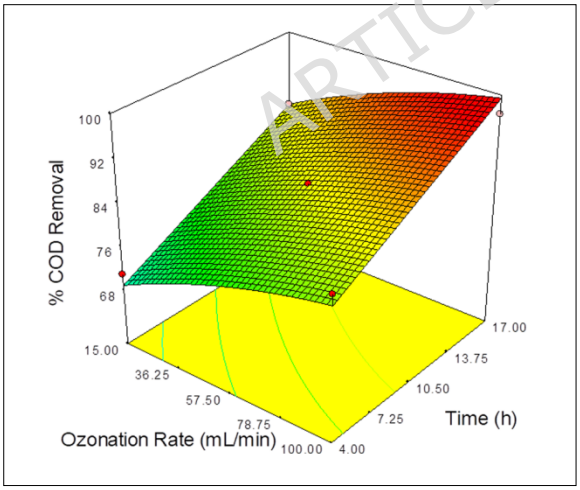

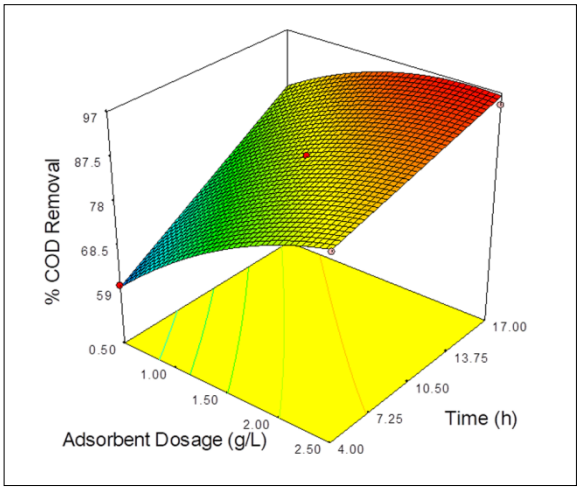

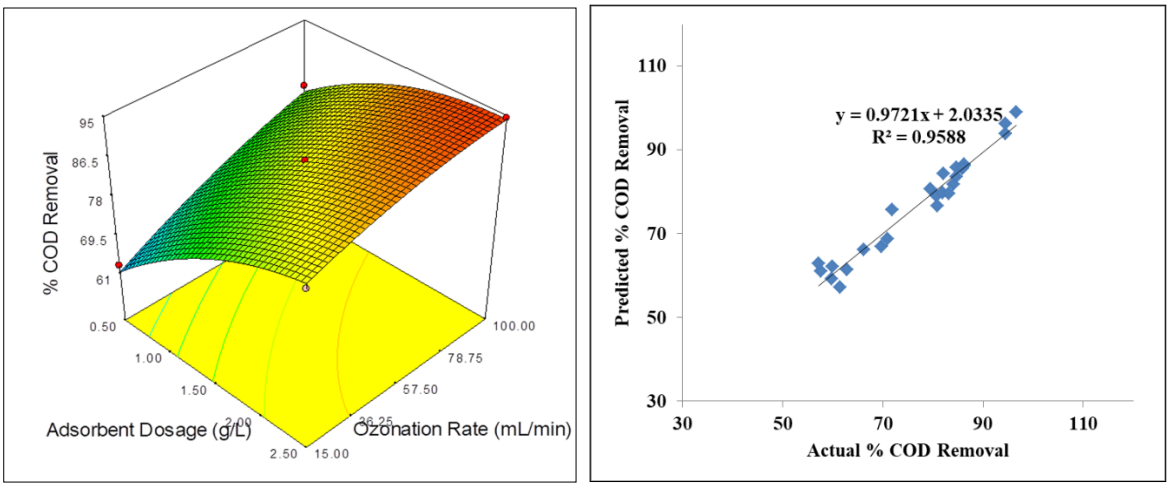

Figure 6 Effect of process variables on % COD removal using KBC

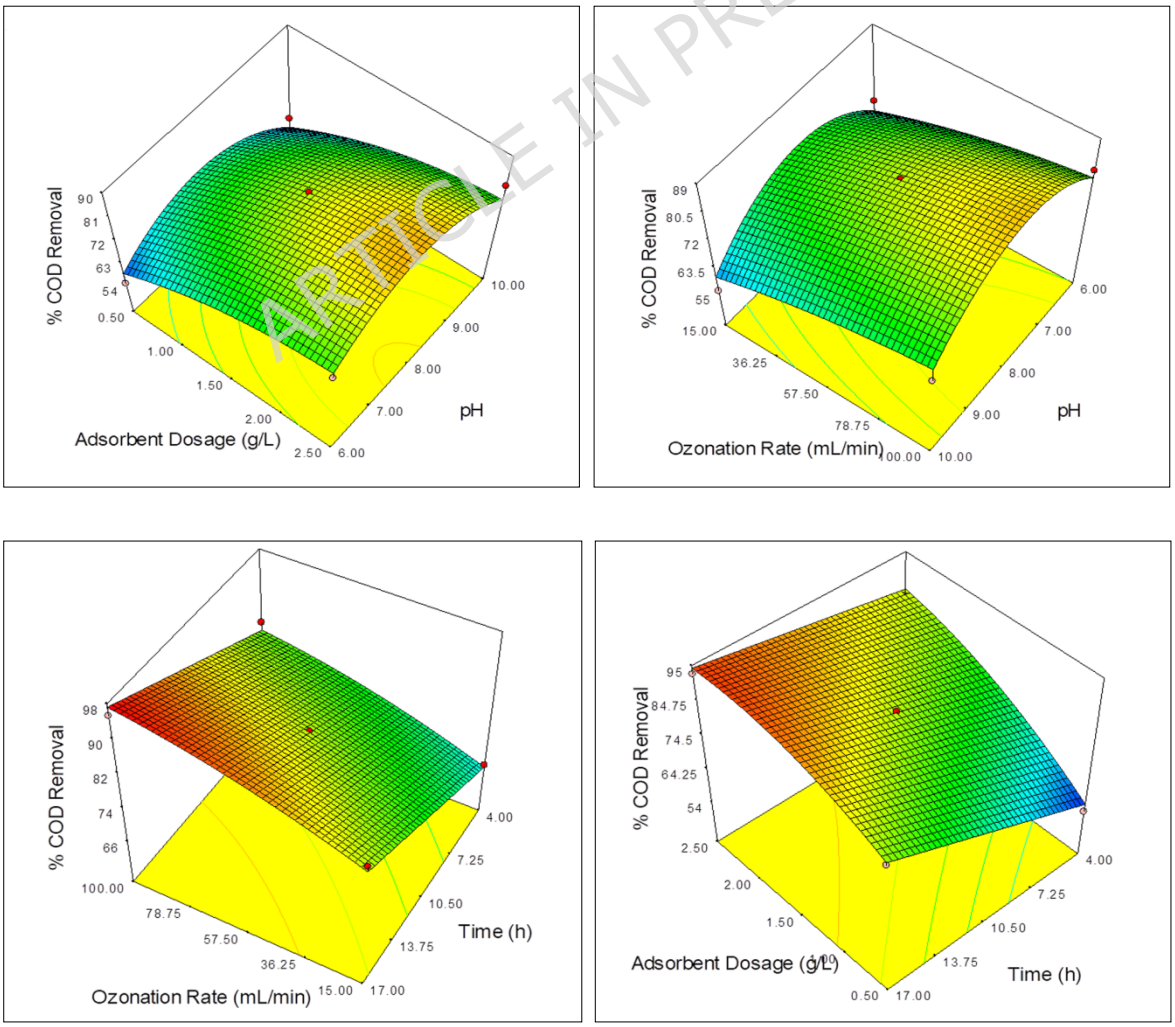

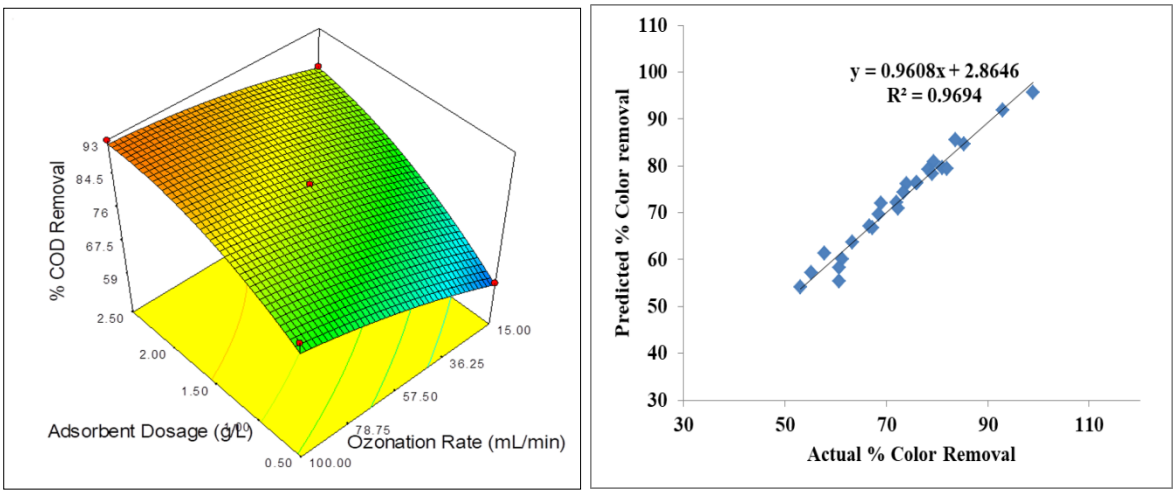

Figure 7 Effect of process variables on % COD removal using NBC

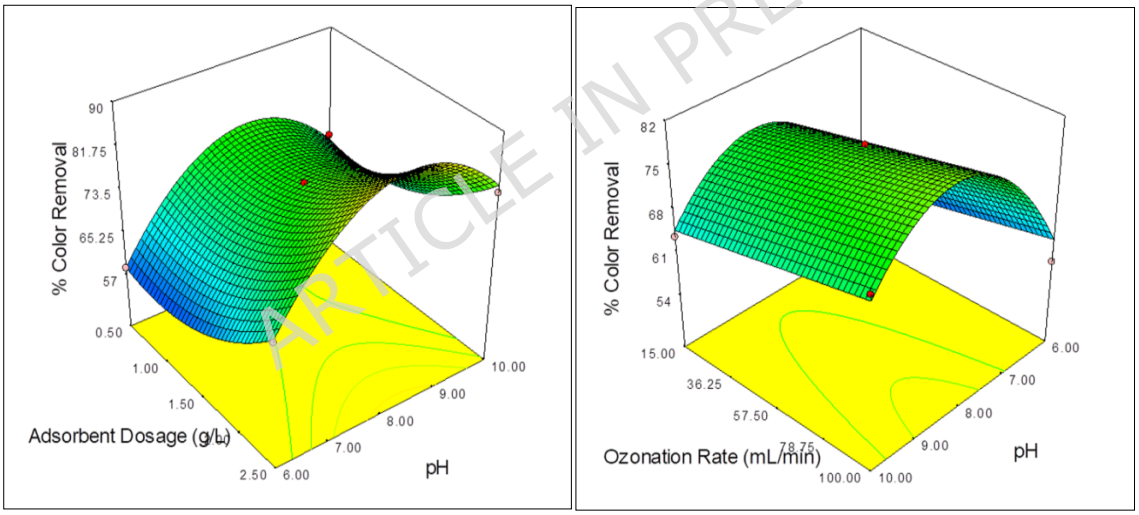

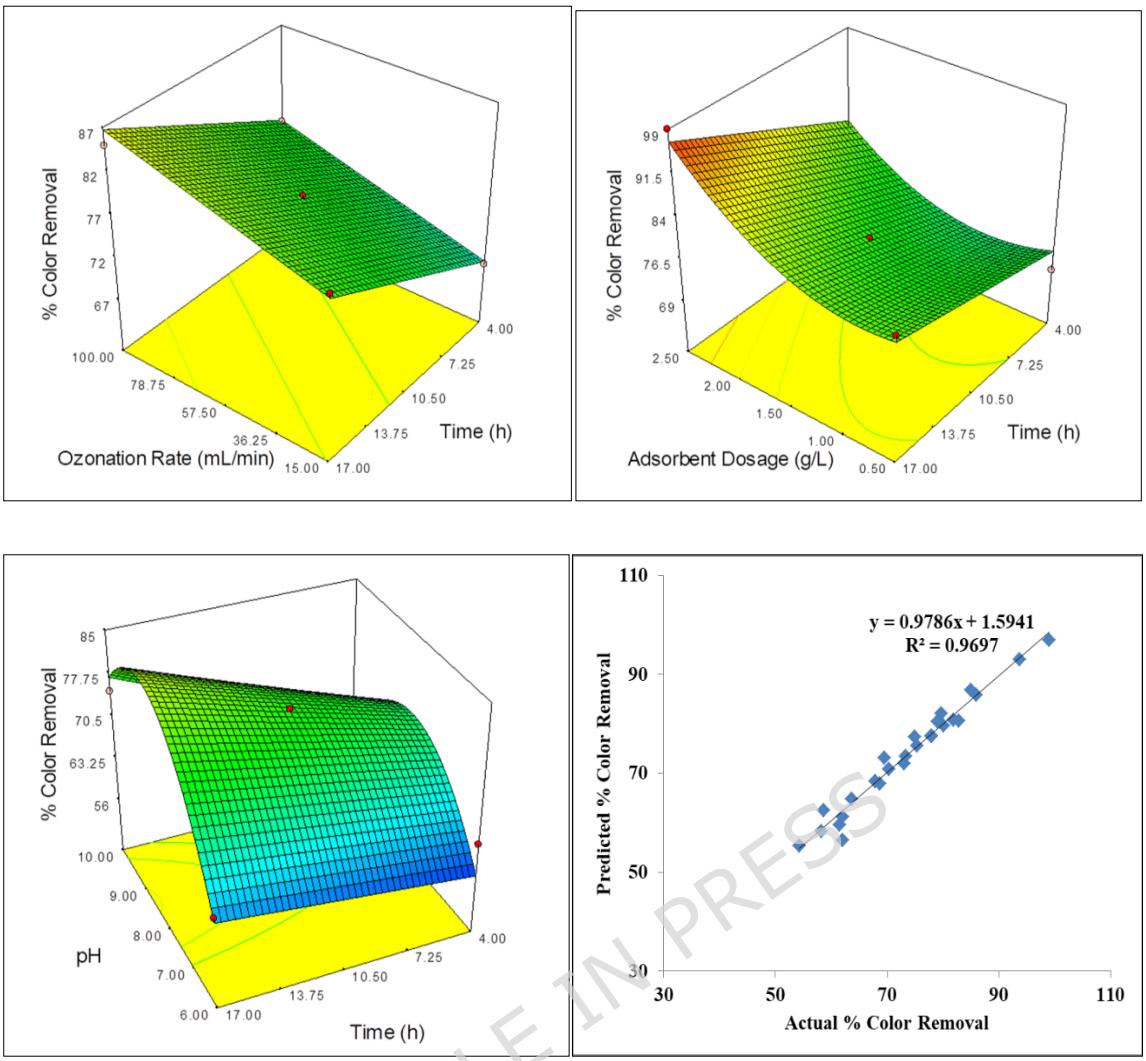

Figure 8 Effect of process variables on % Color removal using KBC

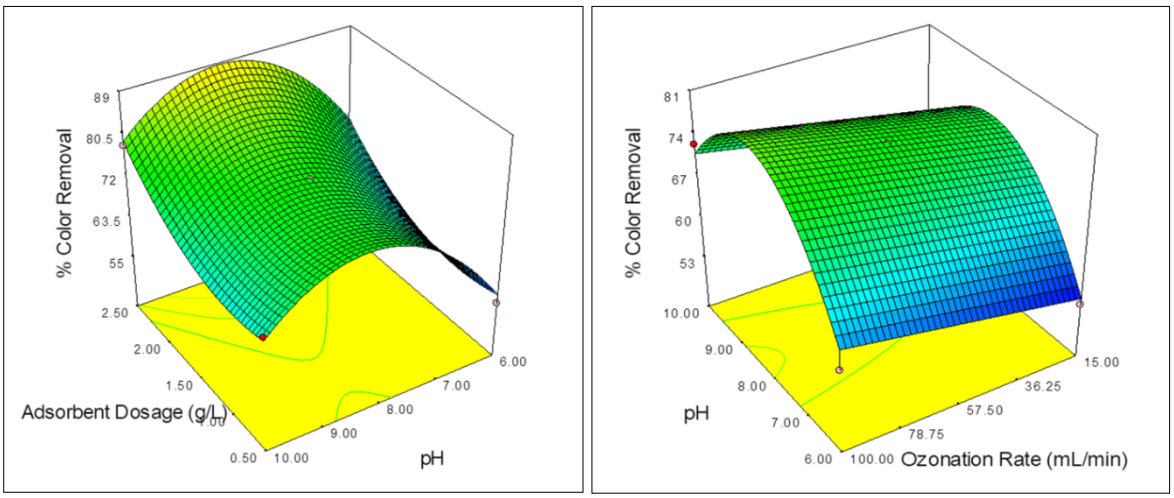

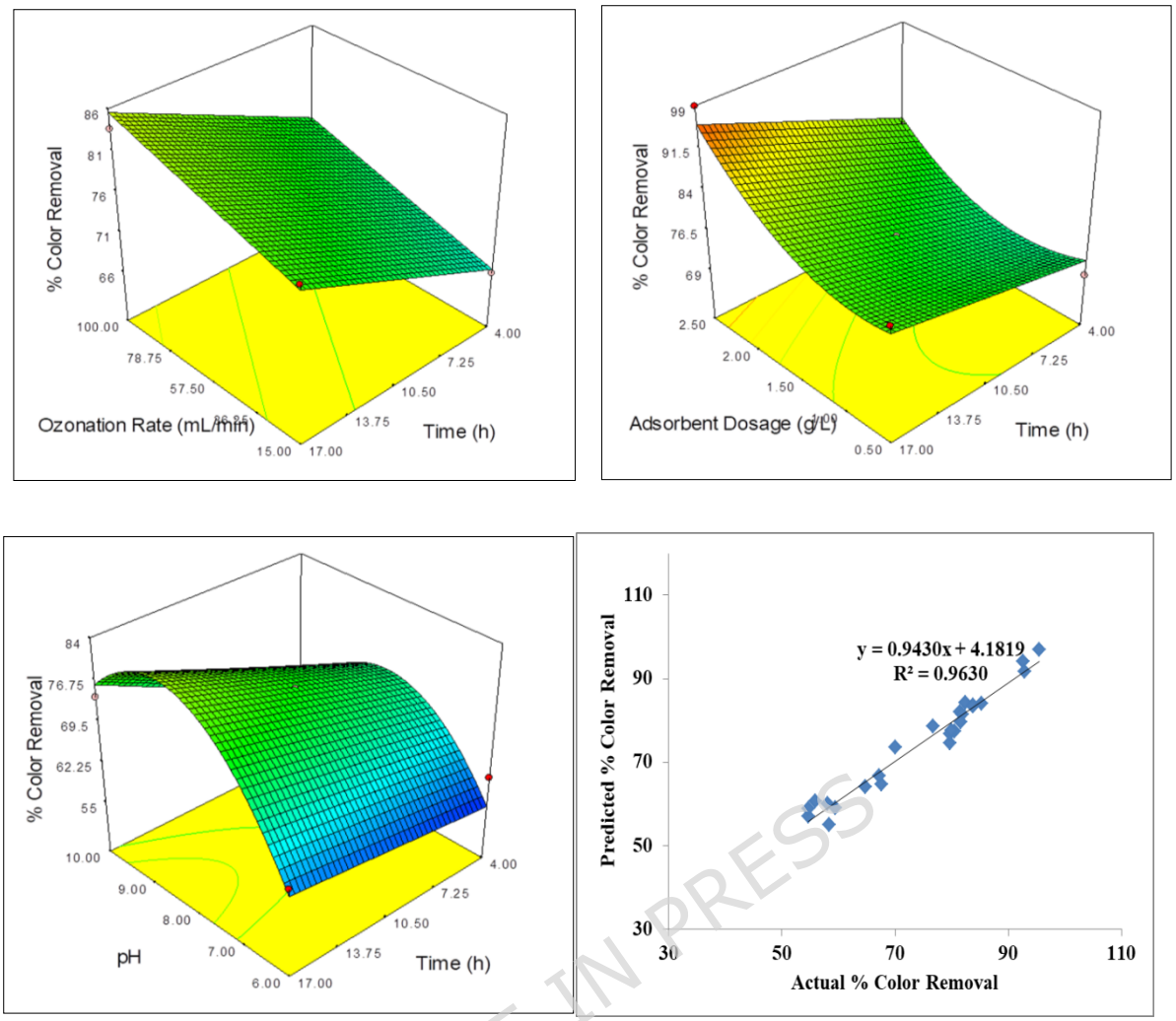

Figure 9 Effect of process variables on % Color removal using NBC

3.4.3 Effect of contact time

The contact period is critical for removing COD and color with KBC and NBC adsorbents. As contact time extended, both Chemical Oxygen Demand and color reduce drastically. After completing the process, the adsorbent and adsorbate are absorbed on the biochar more and more after filtration process [41]. Over time, the rate of removal slowed as adsorption sites were saturated, resulting in a less transfer of mass based on the rate. The saturation time of the content removal for fourteen hours based on the adsorbent dose from 0.5 to 2.5 grams/l, but the dropped started from 9

hours when put the concentration 2.5 gram/l. the new observing detail with another comparable patterns in the adsorption process, from where the effectiveness of reactant to product removal is influenced by both define contact time and proper adsorbent dosage [42].

3.4.4 Effect of Ozonation

Due to its ability to break double bonds and the processes that include ozone and hydroxyl radicals, which are particularly reactive in some situations, ozonation has been shown to be an effective method for getting rid of COD and color, and by adjusting the ozonation rate in combination with adsorption parameters, this study sought to evaluate the impact of ozonation on COD and color removal. Based on adsorption alone was insufficient for successfully eliminating Chemical Oxygen Demand and water color [43]. As the time contact increases based on that the chemical oxygen demand and color change, gives good result in reduction. The reaction based on the bond breaking and new ozone radical bond are attached, after attaching that the organic content reduces. Ozone also caused organic and inorganic pollutants to reach higher oxidation states, which allowed them to be released and further reduced COD. Investigations have shown similar outcomes [44].

The effect of ozonation was found significant with low adsorbent dosage in comparison to high adsorbent dosage, which can be attributed to the high presence of impurities present in the system at low adsorbent dosage. The ozonation may have affected the surface charges of adsorbent enabling the multilayer adsorption which in turn resulted in high adsorption capacity of adsorbent at lower dosage in comparison to higher dosage.

LINEAR VERSUS NON-LINEAR FITTING METHODOLOGY

ADVANTAGES OF LINEAR FITTING:

1. Computational simplicity and widespread availability
2. Facilitates comparison with literature
3. Straightforward parameter estimation

4. Well-established error analysis
5. Transparent calculation process

DISADVANTAGES OF LINEAR FITTING:

1. Linearization may distort error structure
2. Equal weighting regardless of measurement error
3. Potential bias in parameter estimation
4. May not provide best fit
5. Different linearizations yield different parameters

ADVANTAGES OF NON-LINEAR FITTING:

1. Preserves original error structure
2. More accurate parameter estimates
3. Proper data weighting
4. Avoids transformation distortions
5. Unique parameter values

DISADVANTAGES OF NON-LINEAR FITTING:

1. Requires sophisticated software
2. Sensitive to initial parameter guesses
3. Computationally intensive
4. Requires numerical methods expertise
5. Complex error analysis

JUSTIFICATION FOR OUR APPROACH:

Linear fitting selected based on:

- High correlation coefficients ($R^2 > 0.98$)
- Consistency with previous studies for comparison
- Pseudo-second-order model excellent agreement ($R^2 > 0.99$)
- Minimal standard deviations (<5%)

We acknowledge non-linear fitting might provide marginally improved estimates. Future studies could employ both methods.

3.5 Adsorption Kinetic Study

Distinct kinetic models, including pseudo-first order (PFO), pseudo-second order (PSO), and intra-particle diffusion (IPD), were employed to investigate the kinetics of adsorption. The pseudo-first order (PFO) model indicates that the rate of adsorption is directly related to the availability of unoccupied sorption sites or the concentration of ions still present in the solution. The linear form is described by equation (5).

$$\log(q_e - q_t) = \log q_e - \left(\frac{k_1 t}{2.303}\right) \quad (5)$$

The pseudo-second-order (PSO) model includes chemisorption and the equation in linear form is as follows (equation 6)

$$\frac{t}{q_t} = \frac{1}{k_2 q_e^2} + \frac{t}{q_e} \quad (6)$$

The initial rate of intra-particle diffusion is calculated by the intra-particle diffusion (IPD) model and the equation can be expressed as (equation 7):

$$q_t = k_{diff}\ t^{0.5} + C \quad (7)$$

In this instance, qt and qe symbolizes the amount of adsorbate that has been adsorbed at time t and at equilibrium, respectively. The rate constants K_1 and K_2 correspond to the pseudo-first order (PFO) and pseudo-second order (PSO) kinetic models, respectively. K_{diff} (mg/g.min$^{0.5}$) indicates the rate constant for intra-particle diffusion, while t denotes the duration of contact (min). The intercept provides the constant C, which correlates with the thickness of the boundary layer. A greater C value signifies a more pronounced influence of the boundary layer on the adsorption process.

Table 6 Kinetic parameters for real-time textile effluent adsorption onto KBC KOH activated biochar

Model	Initial Conc.	1000			1500			2000			2500		
	Adsorbent dosage (g/L)	0.5	1.5	2.5	0.5	1.5	2.5	0.5	1.5	2.5	0.5	1.5	2.5
PFO	q_{exp}	155.00	57.53	37.60	229.20	84.00	54.20	292.80	109.87	69.68	309.00	129.33	82.32
	k_1 (10^{-3})	4.84	4.84	4.15	5.53	5.07	5.30	5.30	5.07	5.53	5.07	5.07	5.07
	q_{cal}	222.59	70.06	44.44	267.49	84.82	66.08	355.80	128.00	86.46	361.41	144.78	88.92
	R^2	0.9226	0.9449	0.9262	0.9531	0.9522	0.9395	0.9372	0.9410	0.9321	0.9153	0.9143	0.9217
PSO	k_2 (10^{-4})	12.49	63.55	87.35	23.40	79.94	95.51	17.49	47.60	80.15	18.54	48.45	80.14

	q_{cal}	217.39	70.92	46.30	270.27	95.24	63.29	344.83	128.21	80.65	357.14	147.06	92.59
	R^2	0.9975	0.9994	0.9928	0.9992	0.9997	0.9977	0.9978	0.9974	0.9970	0.9966	0.9967	0.9967
	k_{diff}	5.4277	1.8148	1.1720	6.6111	2.2766	1.5589	8.3977	3.1304	1.9461	8.3999	3.4107	2.1372
IPD	C	3.7901	5.3384	2.6199	42.861	19.805	9.5165	52.123	19.824	13.87	65.6190	30.511	20.345
	R^2	0.9776	0.9489	0.9833	0.9151	0.8942	0.9492	0.9483	0.9517	0.9503	0.9568	0.9444	0.9443

Table 7 Kinetic parameters for real-time textile effluent adsorption onto NBC

NaOH activated biochar

Model	Initial Conc.	1000	1500	2000	2500

	Adsorbent dosage (g/L)	0.5	1.5	2.5	0.5	1.5	2.5	0.5	1.5	2.5	0.5	1.5	2.5
PFO	q_{exp}	148.00	55.87	36.80	218.40	82.00	53.20	278.80	107.20	68.40	292.40	125.67	80.40
	k_1 (10^{-3})	5.76	5.30	5.76	5.99	6.22	5.76	5.76	5.76	5.53	5.76	5.30	5.07
	q_{cal}	244.29	77.62	54.88	283.04	115.66	71.25	377.05	149.86	91.26	359.09	148.39	87.92
	R^2	0.9035	0.9286	0.9110	0.9348	0.9256	0.9351	0.9189	0.9053	0.8983	0.9348	0.9145	0.9374
PSO	k_2 (10^{-4})	14.58	55.78	93.30	23.81	57.85	89.02	16.65	43.87	76.96	20.74	49.97	80.29
	q_{cal}	204.08	70.92	46.08	256.41	98.04	63.29	333.33	126.58	79.37	333.33	142.86	90.91
	R^2	0.9965	0.9976	0.9986	0.9989	0.9986	0.9976	0.9977	0.9949	0.9962	0.9987	0.9966	0.9969

	k_{diff}	5.1674	1.8211	1.1862	6.443	2.4581	1.5763	8.2052	3.1294	1.9346	8.1423	3.3301	2.1211
IPD	C	0.87	3.26	2.87	37.57	12.52	8.22	43.47	16.74	12.55	61.32	29.58	19.25
	R^2	0.9675	0.9658	0.9540	0.9129	0.9369	0.9495	0.9518	0.9649	0.9583	0.9321	0.9461	0.9443

Figures 10-12 show the adsorption performance of the PFO, PSO, and IPD models at adsorbent doses of 0.5, 1.5, and 2.5 g/L. Figures 10-12, as well as Tables 5 and 6, show that real-time industrial effluent adsorption is more closely aligned with the PSO model, with a better correlation coefficient (>0.99) than the PFO model (>0.91) for the investigated adsorbent doses and starting concentrations. The predicted maximum adsorption capacity from the PSO model was closer to the experimental values than the PFO model, showing that the adsorption process mostly followed the PSO mechanism. These results show that the adsorption of textile effluent over KOH-activated *Canna indica* charcoal is predominantly controlled by chemisorption rather than physisorption (See Table 7)

The observed maximum adsorption capacities were 309 mg/g for KBC and 292.14 mg/g for NBC, although theoretical estimations anticipated values of 357.14 mg/g and 333.33 mg/g, respectively. The PFO rate constant (k_1) ranged from 4.15×10^{-3} to 5.53×10^{-3}, whereas the PSO rate constant (k_2) varied from 12.49×10^{-4} to 95.51×10^{-4}. These results demonstrate the PSO model's higher prediction accuracy for the kinetics of textile effluent on biochar.

The observed reduction in adsorption capacity at higher doses implies that physisorption is the primary process, whereas at lower dosages, chemisorption takes precedence. The increased adsorption capacity of KBC can be due to its bigger surface area and improved pore dispersion, as proven by BET analysis. Figure 12 depicts two separate stages: effluent diffusion onto the adsorbents' exterior surfaces (KBC and NBC), followed by intraparticle diffusion within the adsorbent surface. The curve's departure from the origin indicates that pore diffusion alone cannot account for the elimination process. KBC has higher correlation coefficients, indicating that its pore distribution and pore radius are more uniform than NBC, which is corroborated by the BET study. The increasing value of C indicates that at

larger concentrations and constant adsorbent doses, the boundary layer effect or surface adsorption (physisorption) becomes more significant, whereas chemisorption takes precedence at lower adsorbent dosages. This conclusion emphasises the role of adsorption dose in determining the relative dominance of physisorption over chemisorption in wastewater treatment.

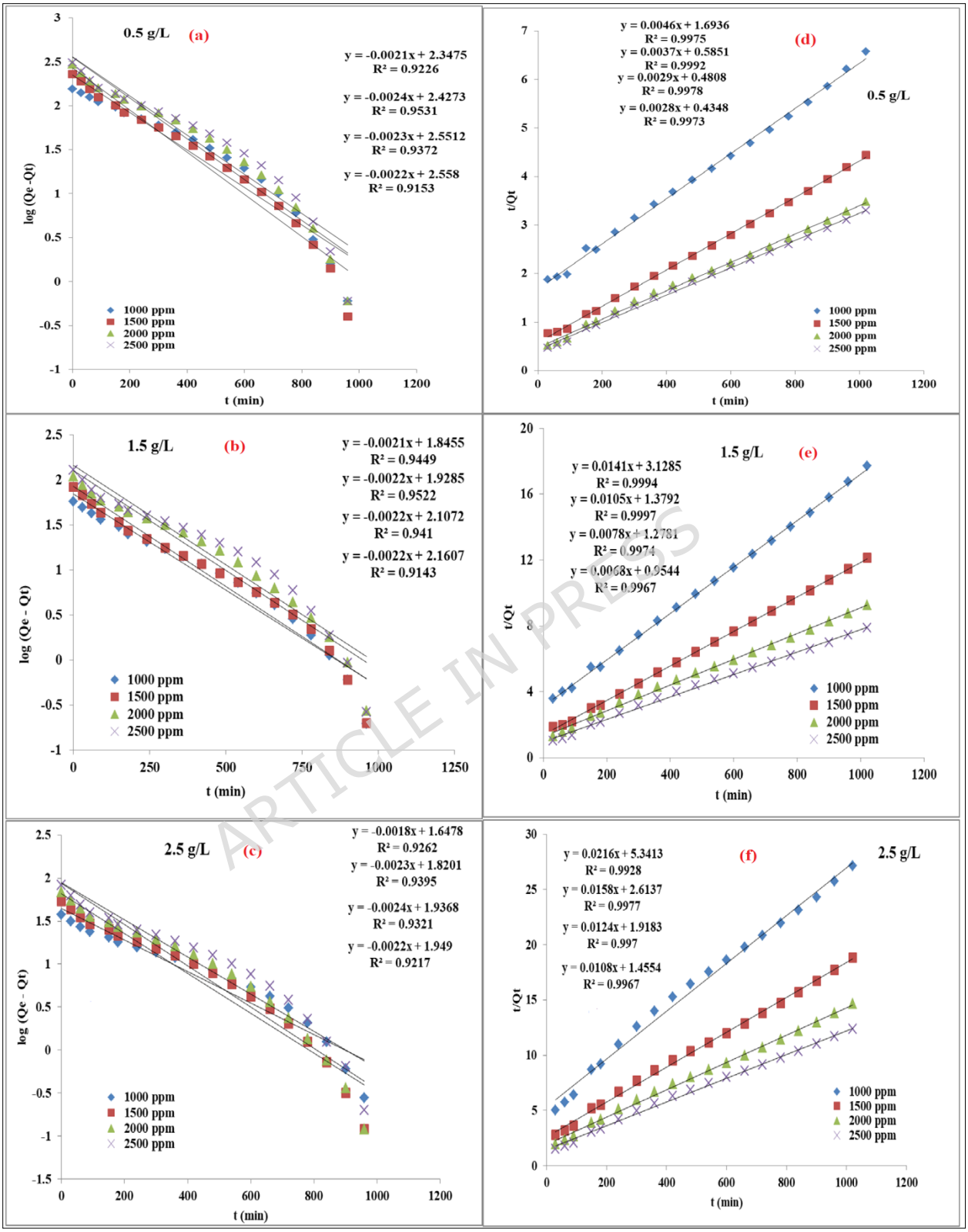

Figure 10 Adsorption Kinetic Models (a, b, c) Pseudo First order (d, e, f) Pseudo Second order for KBC

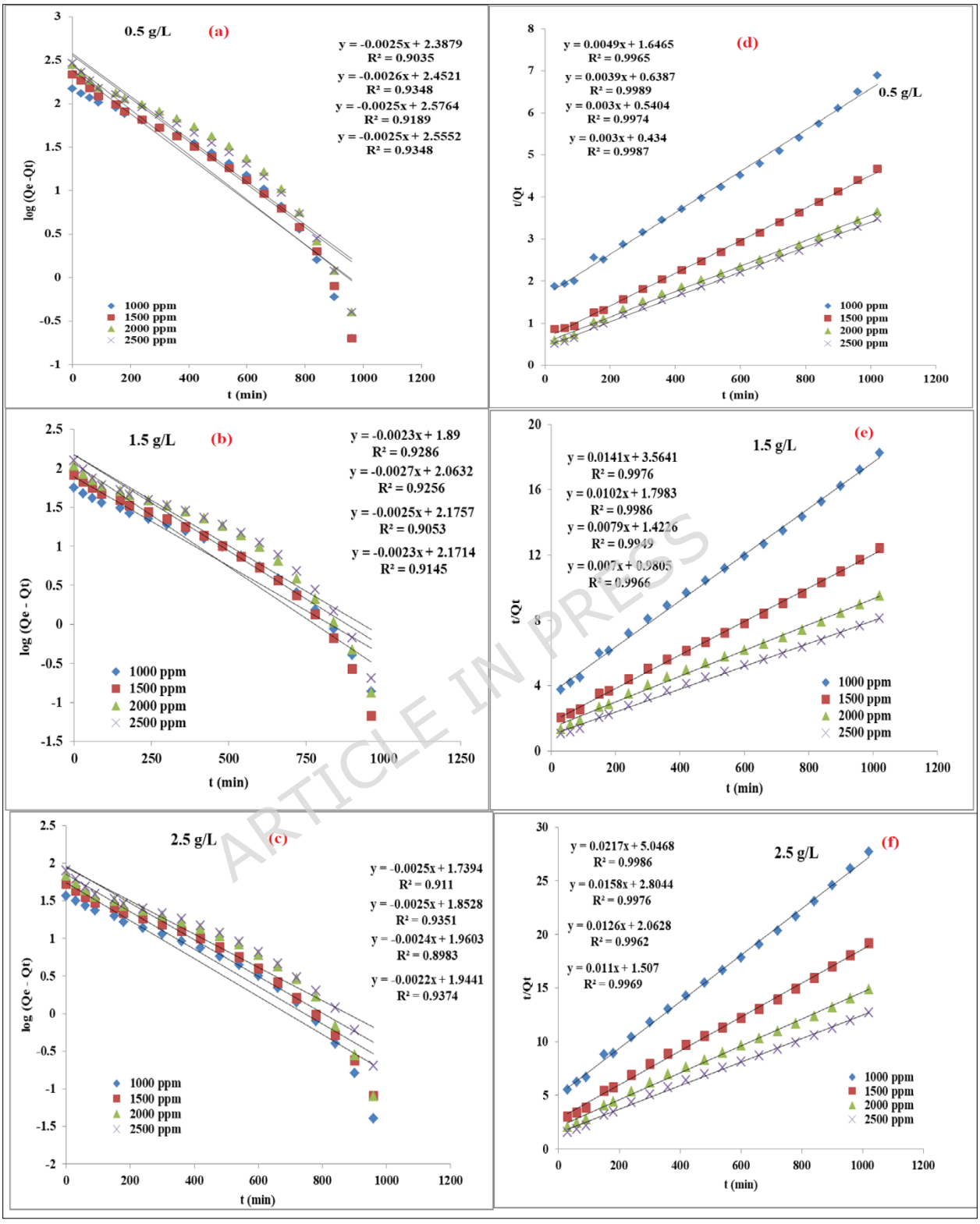

Figure 11 Adsorption Kinetic Models (a, b, c) Pseudo First order (d, e, f) Pseudo Second order for NBC

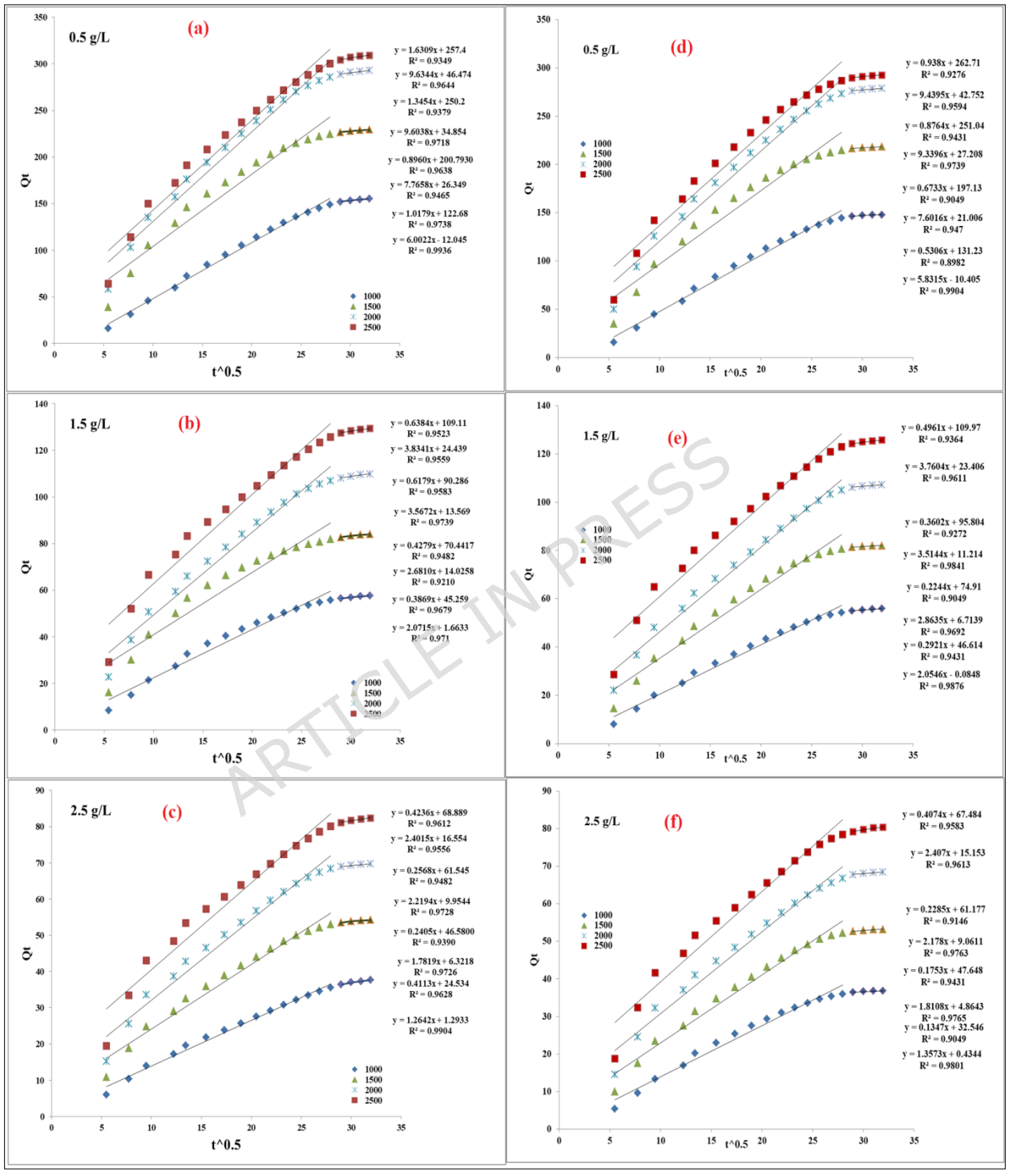

Figure 12 Intra particle diffusion model for KBC (a, b, c) and NBC (d, e, f)

Based on kinetic and isotherm analyses, the adsorption mechanism involves both chemisorption and physisorption processes. The excellent fit to the pseudo-second-order model ($R^2 > 0.99$) indicates that chemisorption is the rate-controlling step, involving chemical interactions between functional groups on the biochar surface and dye molecules. The Langmuir isotherm fit suggests monolayer adsorption on homogeneous sites, while the Freundlich model applicability indicates some degree of surface heterogeneity and multilayer adsorption.

3.6 Adsorption isotherm study

Understanding adsorption behaviour and selecting an appropriate isotherm model are critical for successful COD and color removal from wastewater. These models illustrate how the adsorbate interacts with the aqueous phase and solid adsorbent over time, eventually reaching equilibrium. Various isotherm models, including Langmuir, Freundlich, Temkin, Dubinin-Radushkevich, Elovich, and Halsey, were employed to study the adsorption process on biochar. The best-fitting model was chosen based on the coefficient of determination (R^2), a measure of linear regression accuracy.

The linear form of models employed can be expressed as in equations (8-13):

$$\frac{C_e}{q_e} = \frac{1}{q_m K_L} + \frac{C_e}{q_m} \tag{8}$$

$$\log q_e = \frac{1}{n} \log C_e + \log K_F \tag{9}$$

$$q = \frac{RT}{b}(\ln C_e + \ln K_t) \quad (10)$$

$$\ln q_e = \ln q_m - \beta\varepsilon^2 \quad (11)$$

$$\ln \frac{q_e}{C_e} = -\frac{q_e}{q_m} + \ln K_E q_m \quad (12)$$

$$\log q_e = -\frac{1}{n_H}\ln C_e + \frac{1}{n_H}\ln K_H \quad (13)$$

In this context, qe, qm, and Ce refer to the dye amount adsorbed at equilibrium, the adsorbent's maximum adsorption capacity, and the dye concentration at equilibrium, respectively. The constants KL, KF, n, KT, b, β, KE, KH, and nH correspond to the parameters of the Langmuir, Freundlich, Temkin, D-R, Elovich, and Halsey isotherms. The value of n indicates adsorption intensity, ranging from 1 to 10, which suggests favorable adsorption conditions. R denotes the Universal gas constant, and T represents temperature.

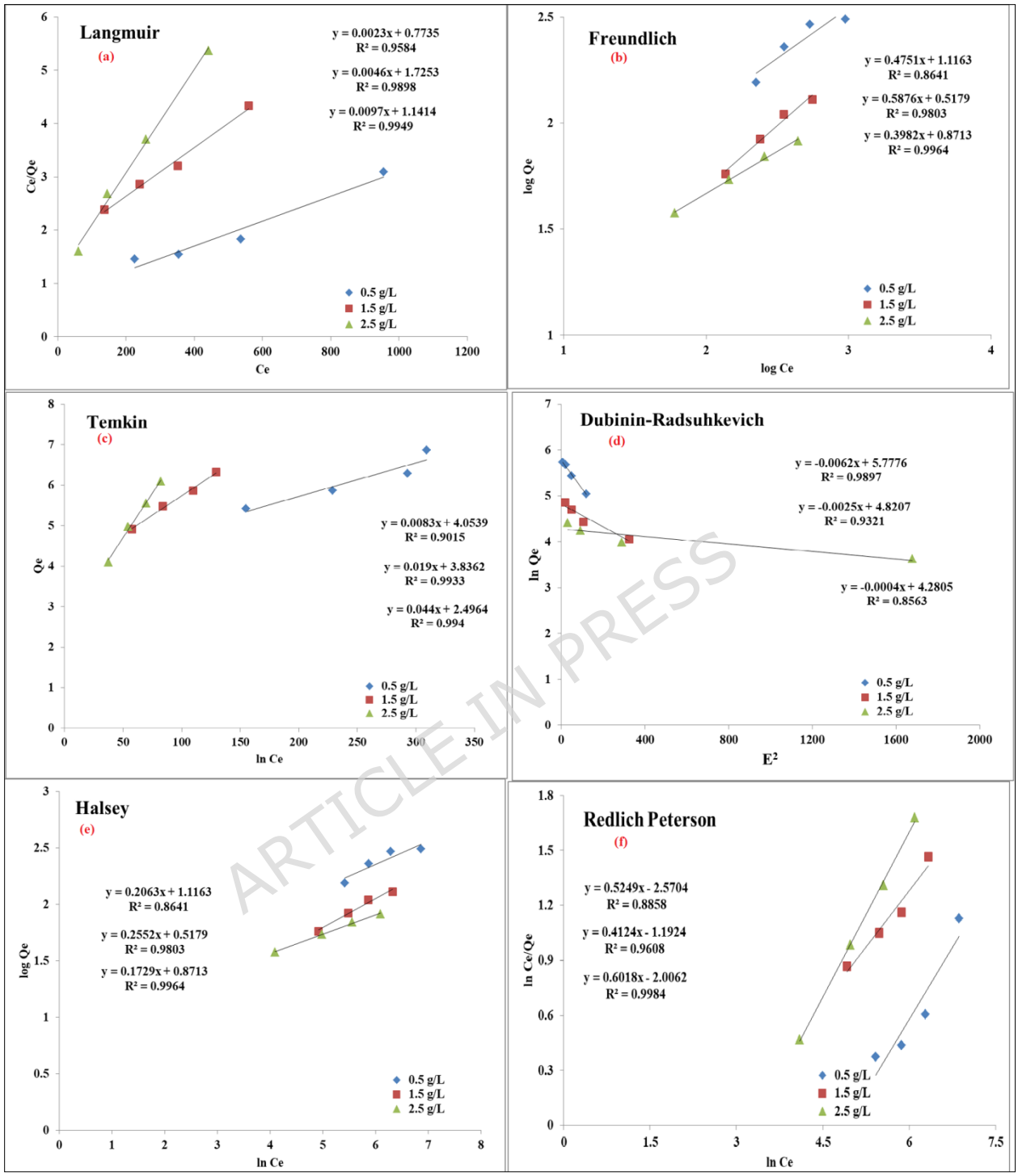

Figure 13 Adsorption isotherm models (a) Langmuir (b) Freundlich (c) Temkin (d) Dubinin-Radushkevich (e) Halsey (f) Redlich-Peterson for KBC

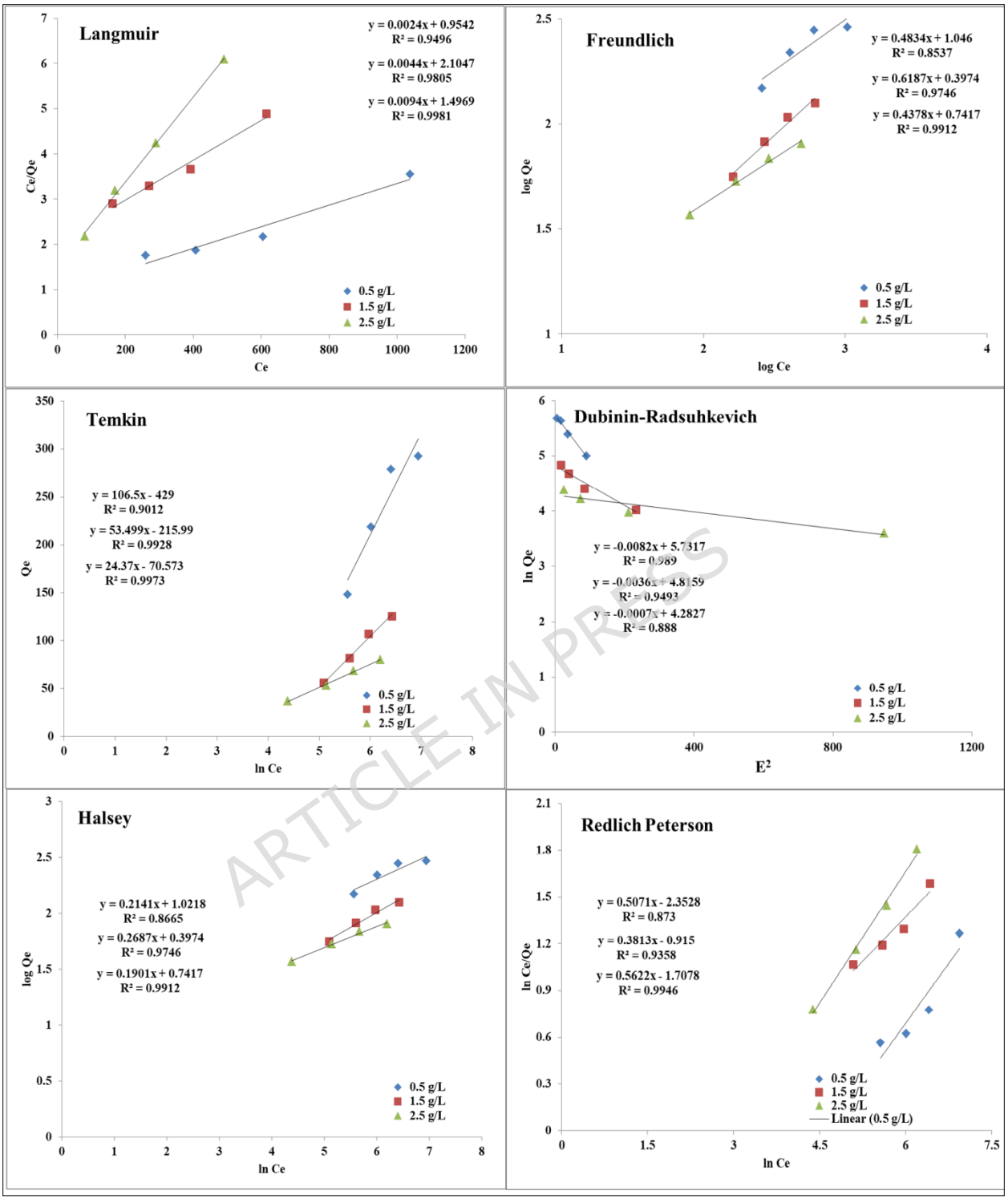

Figure 14 Adsorption isotherm models (a) Langmuir (b) Freundlich (c) Temkin (d) Dubinin-Radushkevich (e) Halsey (f) Redlich-Peterson for NBC

Figures 13 and 14, as well as Table 8, show that the Langmuir isotherm gives the greatest match for the experimental data from KBC and NBC, as evidenced by strong correlation coefficient values. The rise in KL value with increasing adsorbent doses indicates a more intense interaction between the adsorbent and adsorbate. A high R^2 value at increasing adsorbent doses suggests that surface adsorption on homogenous sites occurs more frequently at higher dosages than at lower ones. Furthermore, the Freundlich isotherm's high R^2 value indicates that multilayer adsorption helps to remove COD and color from the solution. The rising value of n indicates that as the adsorbent dose increases, so does the adsorption intensity. Similarly, a rise in KT suggests that with a constant adsorbate concentration, the binding energy between the adsorbent and adsorbate strengthens as the adsorbent dosage increases. The adsorption capacity calculated using Langmuir suggested that the KBC is better than NBC which is supported by other isotherms used for the analysis. The high R^2 of DR at the low adsorbent dosage suggested that micro-porous adsorption of impurities is prevalent in comparison to a higher dosage of adsorbent. The mean adsorption energy value suggested that chemisorption is dominant which is supported by kinetic analysis. The order of significance for isotherms based on R^2 is found as Langmuir > Temkin > Redlich-Peterson > Freundlich = Halsey > Dubinin-Radushkevich for KBC whereas Langmuir > Temkin > Halsey > Freundlich > Dubinin-Radushkevich > Redlich-Peterson for NBC.

Table 8 Isotherm parameters and their values for KBC and NBC

Isotherm model		KBC			NBC		
		0.5	1.5	2.5	0.5	1.5	2.5
Langmuir	q_m	434.78	217.39	103.09	416.67	227.27	106.38
	k_L (10^{-3})	2.67	2.97	8.50	2.29	9.26	14.07
	R^2	0.9584	0.9898	0.9949	0.9501	0.9805	0.9981
Freundlich	n	2.10	1.70	2.51	2.07	1.62	2.28
	k_F	13.09	3.30	7.44	11.11	2.50	5.52
	R^2	0.8636	0.9803	0.9964	0.8548	0.9746	0.9912
Temkin	b	22.91	47.48	109.70	23.27	46.31	101.66
	k_T	0.0217	0.0218	0.0837	0.0178	0.0176	0.0552
	R^2	0.9012	0.9933	0.9940	0.9026	0.9928	0.9973
DR	β	0.0062	0.0025	0.0004	0.0082	0.0036	0.0007
	q_m	323.05	124.05	72.28	308.34	123.46	72.44
	R^2	0.9900	0.9321	0.8563	0.9893	0.9493	0.8880
Halsey	n_H	-4.85	-3.92	-5.78	-4.67	-3.72	-5.26
	k_H	0.0045	0.1314	0.0065	1.24	0.23	0.02
	R^2	0.8636	0.9803	0.9964	0.8677	0.9746	0.9912
	β	0.5250	0.4124	0.6018	0.5072	0.3813	0.5622

Redlich Peterson	A	13.09	3.29	7.44	10.51	2.50	5.52
	R^2	0.8855	0.9608	0.9984	0.8741	0.9358	0.9946

Industrial textile effluents contain high concentrations of organic pollutants that significantly increase COD levels. Without effective treatment, these noxious compounds from dyes can persist in receiving water bodies, causing environmental degradation and potential health risks (Wang et al., 2024; Liu et al., 2022; Xu et al., 2024).

Response surface optimization of process parameters has comparative advantages over linear optimization approaches, as the outputs are comprehensive and effective for interpreting multiple parameter interactions simultaneously (refs).

3.7 Response Surface Methodology

In this study, the Response Surface Methodology-Box Behnken Design (RSM-BBD) was used to evaluate how various parameters affect COD and color removal from wastewater. The process factors adsorbent dose, pH, contact duration, ozonation rate, and type of activated charcoal were adjusted at different levels to determine their individual and combined impacts on COD and color removal efficiency. Table 5 shows the experimental setup, which contained four numerical variables and one categorical variable, as well as the actual and coded data. To assess the impact of these factors in the removal process, a quadratic model was created using the design matrix. The empirical link between the process variables (adsorbent dose, pH, ozonation rate, contact duration, and biochar type) and the responses (percentage of COD removal and color removal) was derived using the experimental data presented in Tables 8 and 9, as shown in equations (14-19) in both coded and actual formats.

SYNERGISTIC INTERACTIONS BETWEEN PROCESS VARIABLES

1. ADSORBENT DOSE × pH: Strong positive synergy at optimal pH (7-8 for KBC, 8-9 for NBC). At suboptimal pH, increased dose effect is diminished.

2. CONTACT TIME × ADSORBENT DOSE: Synergistic relationship in intermediate range. Low dose requires extended time (>15h); high dose needs shorter time (8-10h).

3. OZONATION RATE × ADSORBENT DOSE: Antagonistic interaction. At low dose (0.5-1.0 g/L), ozonation provides 15-20% improvement. At high dose (>2.0 g/L), benefit decreases to 5-8%, suggesting adsorption dominance.

4. pH × OZONATION RATE: Complex interaction. At alkaline pH (8-10), ozonation more effective due to enhanced ·OH radical formation. Optimal combination: pH 8-10 with 50-70 mL/min.

5. CONTACT TIME × OZONATION: Extended time (>12h) with continuous ozonation shows diminishing returns. Optimal: 8-12h contact with 50-70 mL/min ozonation.

These interactions justify using RSM-BBD for simultaneous multi-parameter optimization.

$$\begin{aligned}\text{COD Reduction (\%)} &= 84.63 - 2.01(\text{pH}) + 9.81(\text{AD}) + 6.61(\text{OR}) + 8.69(\text{CT}) \\ &\quad - 2.41(\text{AD} \times \text{OR}) - 3.81(\text{AD} \times \text{CT}) - 12.68(\text{pH})^2 - 3.99(\text{AD})^2 \\ &\quad - 1.56(\text{OR})^2 - 1.09(\text{BT})\end{aligned} \tag{14}$$

$$\text{COD Removal}(\%) = 76.94 + 4.78(\text{pH}) + 6.26(\text{AD}) + 3.59(\text{OR}) + 5.64(\text{CT}) - 1.82(\text{AD} \times \text{CT}) + 3.26(\text{pH} \times \text{CT}) - 13.88(\text{pH})^2 + 5.68(\text{AD} - 0.60(\text{BT}) \quad (15)$$

An empirical equation for COD reduction (%) in terms of actual factors for KOH (equation 16) and NaOH (equation 17) as given below

$$\text{COD Reduction}(\%) = -172.6831 + 49.6978(\text{pH}) + 31.1852(\text{AD}) + 0.3398(\text{OR}) + 2.2163(\text{CT}) - 0.5862(\text{AD} \times \text{CT}) - 0.0567(\text{AD} \times \text{OR}) - 3.1690(\text{pH})^2 - 3.9861(\text{AD})^2 - 0.0009(\quad (16)$$

$$\text{COD Reduction}(\%) = -174.8655 + 49.6978(\text{pH}) + 31.1852(\text{AD}) + 0.3398(\text{OR}) + 2.2163(\text{CT}) - 0.5862(\text{AD} \times \text{CT}) - 0.0567(\text{AD} \times \text{OR}) - 3.1690(\text{pH})^2 - 3.9861(\text{AD})^2 - 0.0009(\text{OR})^2 \quad (17)$$

An empirical equation in terms of actual factors for KOH (equation 18) and NaOH (equation 19) as given below

$$\text{COD Removal}(\%) = -148.6881 + 55.2640(\text{pH}) - 13.7349(\text{AD}) + 0.0844(\text{OR}) - 1.5605(\text{CT}) + 0.2509(\text{pH} \times \text{CT}) + 0.2804(\text{AD} \times \text{CT}) - 3.4691(\text{pH})^2 + 5.6822(\text{AD})^2 \quad (18)$$

$$\text{COD Removal}(\%) = -149.8808 + 55.2640(\text{pH}) - 13.7349(\text{AD}) + 0.0844(\text{OR}) - 1.5605(\text{CT}) + 0.2509(\text{pH} \times \text{CT}) + 0.2804(\text{AD} \times \text{CT}) - 3.4691(\text{pH})^2 + 5.6822(\text{AD})^2 \quad (19)$$

Table 9 ANOVA Table for % COD Removal (% CODR)

Source	Sum of Squares	Contribution	Degree of Freedom	Mean Squares	F-value	p-Value Prob>F
Model	7722.85	96.11	10	772.29	116.13	< 0.0001
AD	2310.45	29.22	1	2310.45	347.42	< 0.0001
pH	97.28	1.23	1	97.28	14.63	0.0004
OR	1047.82	13.25	1	1047.82	157.56	< 0.0001
CT	1812.73	22.92	1	1812.73	272.58	< 0.0001
BT	69.06	0.87	1	69.06	10.38	0.0023
AD*OR	46.46	0.59	1	46.46	6.99	0.0111

AD*CT	116.13	1.47	1	116.13	17.46	0.0001
AD^2	213.78	2.70	1	213.78	32.15	< 0.0001
pH^2	2161.93	27.34	1	2161.93	325.08	< 0.0001
OR^2	32.74	0.41	1	32.74	4.92	0.0314
Residual	312.57	3.89	47	6.65		
Lack of Fit	312.57		39	8.01		
Pure Error	0.00		8	0.00		
Cor. Total	8035.42		57			

R^2 = 0.9611; Adj. R^2 = 0.9528; Pred. R^2 = 0.9405; Ad. Prec. = 39.54; C.V% = 3.35

ADEQUACY OF MODEL PREDICTION

Adequate precision (Adeq. Prec.) measures signal-to-noise ratio; values >4 indicate adequate model discrimination.

For % COD Removal Model:

Adequate precision = 39.54 (Table 9) - approximately 10× greater than threshold of 4. This indicates excellent signal-to-noise ratio and confirms reliable COD removal prediction across entire experimental range.

For % Color Removal Model:

Adequate precision = 51.39 (Table 10) - nearly 13× greater than required threshold. This exceptionally high value demonstrates superior model adequacy and predictive capability.

Both models significantly exceed minimum requirement, validating suitability for:

(i) Predicting responses at untested variable combinations

(ii) Optimizing process conditions for maximum removal

(iii) Understanding variable-response relationships

(iv) Industrial scale-up applications

High adequate precision values, combined with high R^2 (0.9611 for COD, 0.9696 for color) and low CV% (3.35% for COD, 2.73% for color), demonstrate excellent model fitness and reliability.

Table 10 ANOVA table for % Color Removal (% COLR)

Source	Sum of Squares	Contribution	Degree of Freedom	Mean Squares	F-value	P-value Prob>F
Model	6159.58	96.96	9	684.40	169.84	< 0.0001
AD	939.25	16.21	1	939.25	233.08	< 0.0001

pH	549.32	9.45	1	549.32	136.32	< 0.0001
OR	308.67	5.33	1	308.67	76.60	< 0.0001
CT	762.19	13.15	1	762.19	189.15	< 0.0001
BT	20.63	0.36	1	20.63	5.12	0.0282
AD*CT	26.57	0.46	1	26.57	6.59	0.0134
pH*CT	85.09	1.7	1	85.09	21.11	< 0.0001
AD^2	445.70	7.69	1	445.70	110.60	< 0.0001
pH^2	2658.05	45.86	1	2658.05	659.62	< 0.0001
Residual	193.42	3.04	48	4.03		
Lack of Fit	193.42		40	4.84		
Pure Error	0.00		8	0.00		
Cor. Total	6353.00		57			

R^2 = 0.9696; Adj. R^2 = 0.9638; Pred. R^2 = 0.9474; Ad. Prec. = 51.39; C.V% = 2.73

Table 1 shows that the projected values from the RSM-BBD quadratic model closely match the experimental data. The ANOVA findings in Tables 9 and 10 indicate that the models are sufficient and statistically significant. The high F-values for percent COD elimination (116.13) and percent color removal (169.84) highlight the model's statistical validity. A p-value of less than 0.0001 implies that both % COD elimination and % color removal is highly significant. The model's accuracy was confirmed by coefficients of determination (R^2) and adjusted R^2 values of 0.9611 and 0.9528 for COD removal, and 0.9696 and 0.9638 for color removal. Furthermore, the low coefficient of variation values for both responses (3.35% for COD and 2.79% for color) suggest that the model is consistent and reliable as indicated by equations (x-xv). ANOVA analysis [20-21] shows that linear terms like adsorbent dosage (AD), pH, ozonation rate (OR), contact time (CT), and biochar type (BC), as well as quadratic terms like AD^2, pH^2, and OR^2, and cross-product terms like ADOR and ADCT, are statistically significant with p-values below 0.05. The most important parameters for % COD and % COL elimination was found to be adsorbent dose, pH, and contact duration.

The optimal parameters for % COD and % COL removal was statistically predicted as follows: for NBC, an adsorbent dosage of 2.5 g/L, pH 8.25, an ozonation rate of 67.56 mL/min, and a contact length of 17 hours resulted in 96.88% COD R and 98.57% COL R, with 98.57% desirability. KBC's characteristics were an adsorbent dosage of 2.5 g/L, a pH of 8.21, an ozonation rate of 79.48 mL/min, and a contact length of 17 hours, yielding 95.66% COD R and 98.23% COL R with 98% desirability. The experimental

validation showed that NBC had 94.33% COD R and 93.6% COL R, whereas KBC had 93.76% COD R and 95.4% COL R.

BBD vs CCD Justification

Box-Behnken Design (BBD) was selected over Central Composite Design (CCD) due to its efficiency in reducing the number of experimental runs while maintaining adequate prediction capability. BBD is particularly suitable for exploring quadratic response surfaces and requires fewer corner points, making it more economical for multi-factor optimization studies (refs).

Linear vs Non-linear Fitting Justification

Linear fitting was employed for kinetic and isotherm models due to its simplicity and widespread acceptance in literature, facilitating comparison with previous studies. While non-linear fitting might provide marginally better fits, the high correlation coefficients ($R^2 > 0.99$ for PSO model) obtained with linear fitting demonstrate excellent model adequacy for describing the adsorption behavior.

3.8 Adsorption Mechanism

COMPREHENSIVE ADSORPTION MECHANISM

1. ELECTROSTATIC ATTRACTION: At optimal pH (7-9), negative surface charges (-COO^-, -O^-) attract cationic dyes through Coulombic forces

2. π-π INTERACTIONS: Aromatic biochar structure enables π-π stacking with aromatic dye molecules

3. HYDROGEN BONDING: Abundant -OH and -COOH groups form H-bonds with dye molecules

4. PORE FILLING: Mesoporous structure (2.85-3.12 nm pores) accommodates dye molecules (1-3 nm) through diffusion and van der Waals forces

5. ION EXCHANGE: Ionic functional groups exchange with ionic species ($Na^+/K^+ \leftrightarrow$ cationic dyes)

6. COMPLEXATION: Oxygen-containing groups form coordination complexes with metal ions

7. SYNERGISTIC OZONATION MECHANISM:

a) Direct ozonation: O_3 attacks electron-rich sites (C=C, aromatic rings)

b) Indirect oxidation: $O_3 \rightarrow \cdot OH$ radicals at alkaline pH

c) Surface-catalyzed oxidation: Biochar catalyzes O_3 decomposition

d) Desorption prevention: Continuous oxidation creates new sites

[FIGURE 15: Schematic diagram will be inserted showing all mechanisms at molecular level, biochar cross-section with porous structure, ozone interaction, before/after treatment comparison]

Mechanism dominance varies with conditions:

- Low pH (<5): Ion exchange and pore filling
- Neutral pH (6-8): Electrostatic attraction, H-bonding, π-π interactions
- High pH (>9): Oxidative degradation compensates for electrostatic repulsion

Pseudo-second-order kinetics ($R^2 > 0.99$) indicate chemisorption is rate-limiting. Langmuir isotherm fit suggests monolayer adsorption on homogeneous sites.

Conclusion

This study assessed the efficacy of adsorption followed by ozonation in treating wastewater from a working textile mill to remove color and COD. The findings imply that *Canna indica* may be used as an excellent adsorbent in the adsorption process to remove dyes and chemical oxygen requirement. KOH-activated biochar at a 1.5 g/L adsorbent dose resulted in 99% color removal and a 96.67% decrease in COD. The RSM-BBD study demonstrated that pH had a substantial impact on the adsorption process and subsequent ozonation for COD and color removal. KOH-activated biochar (KBC) had a maximum adsorption capacity of 357.14 mg/g, exceeding non-activated biochar (NBC) with a capacity of 333.33 mg/g. KOH-treated biochar outperformed NaOH-treated biochar in terms of adsorption capacity. pH was shown to be more important than adsorbent dose, duration, and ozonation rate. Langmuir > Temkin > Redlich-Peterson > Freundlich = Halsey > Dubinin-Radushkevich is the order of importance for isotherms in KBC, but in NBC, it is Langmuir > Temkin > Halsey > Freundlich > Dubinin-Radushkevich > Redlich-Peterson.

Future Work:

- Post-adsorption SEM analysis will also work to gain a more comprehensive understanding of the changes in surface morphology.
- Post-adsorption EDX mapping will also enhance mechanistic insight into elemental distribution and strengthen the scientific depth of the study

REGENERATION AND ECONOMIC VIABILITY

We acknowledge regeneration and reusability studies are critical for economic feasibility. Current study focused on proof-of-concept and optimization; regeneration planned for future work.

PROPOSED REGENERATION METHODS:

1. THERMAL: Heating at 300-500°C under inert atmosphere
2. CHEMICAL: Treatment with 0.1 M NaOH or organic solvents
3. COMBINED: Ozonation + mild thermal treatment
4. BIOLOGICAL: Microbial degradation in subsequent bioreactor

PRELIMINARY ECONOMIC ASSESSMENT:

Even without regeneration, process offers advantages:

- Canna indica is waste biomass (zero feedstock cost)
- KOH/NaOH activation chemicals inexpensive (₹50-80/kg)
- Biochar yield 30-57% - substantial adsorbent from limited biomass
- Reduced ozone consumption vs standalone (50-70 vs 150-200 mL/min)
- Achieves >96% COD and >98% color removal, meeting discharge standards

FUTURE RESEARCH PRIORITIES:

1. 5-cycle regeneration studies to assess degradation
2. Life cycle assessment (LCA) vs conventional treatment
3. Cost-per-cubic-meter calculation including regeneration
4. Optimal regeneration condition investigation
5. Environmental impact assessment of regeneration waste

Recent biochar regeneration studies suggest 4-6 cycles possible with <20% capacity loss.

Authors contributions:

V.K.U.S. (Vishal Kumar U. Shah) contributed to conceptualization, methodology development, experimental investigation, data collection, and preparation of the original manuscript draft.

P.G. (Pratima Gajbhiye) contributed to conceptualization, supervision of the research work, validation of experimental results, and review and editing of the manuscript.

A.M.Y. (Anand Mohan Yadav) contributed to experimental support, formal data analysis, validation of results, and interpretation of experimental findings.

J.B.T. (Jay B. Trivedi) contributed to methodological guidance, technical input related to adsorption processes, and critical review of the experimental methodology.

A.S. (Aparna Singh) contributed to data interpretation, validation of analytical results, and manuscript review and editing.

A.P. (Aditee Pandya) contributed to analytical support related to wastewater characterization, validation of experimental data, and manuscript review.

M.I.H.S. (Md. Irfanul Haque Siddiqui) contributed to scientific review, technical guidance, and critical evaluation of the manuscript.

C.K.C. (Choon Kit Chan) contributed to formal analysis, validation of experimental findings, and manuscript review and editing.

S.D. (Saurav Dixit) contributed to resources, data interpretation support, and manuscript review.

A.Pa. (Anand Patel) contributed to validation of results, technical inputs, and review and editing of the manuscript.

X.Y. (Xu Yong) contributed to scientific supervision, critical revision of the manuscript, improvement of scientific interpretation of results, and guidance during the revision process including responses to reviewer comments.

All authors reviewed and approved the final version of the manuscript.

All authors meet the authorship criteria of the journal, have made meaningful contributions to the study, and have approved the final version of the manuscript as well as the revised authorship list.

Conflict of interests:

There is no conflict of interests among authors

Acknowledgement:

The authors extend their appreciation to the **Guanxi science and Technology program (AA24010001) &** Researchers Supporting Project number (RSPD2025R999), King Saud University, Riyadh, Saudi Arabia.

Data Availability:

The datasets used and/or analyzed during the current study available from the corresponding author Xu Yong on reasonable request

References

1. Kriaa, K., Gataa, I. S., Mostafa, L., Shaban, M., Hussein, Z. A., Singh, N. S. S., Sadeq, A. M., & Hajlaoui, K. (2025). Computational artificial intelligence application in UF membrane operational behavior assessment for wastewater treatment. *Journal of Water Process Engineering, 76*, 108290. https://doi.org/10.1016/j.jwpe.2025.108290
2. Akbar, NA., & Sabri, S., Bakar, AA., & Azizan, NS., (2019) *Removal of color using banana stem adsorbent in textile wastewater*. In Journal of Physics: Conference Series (Vol. 1349:1, 012091). IOP Publishing. DOI: - https://doi.org/10.1088/1742-6596/1349/1/012091
3. Tan, W., Wang, L., Yu, H., Zhang, H., Zhang, X., Jia, Y., & Xi, B., (2019) *Accelerated microbial reduction of azo dye by using biochar from iron-rich-biomass pyrolysis*. Materials, 12:7, 1079. https://doi.org/10.3390/ma12071079
4. Khaled, A., Nemr, AE., Sikaily, AE., & Abdelwahab, O., (2009) *Removal of Direct N Blue-106 from artificial textile dye effluent using activated carbon from orange peel: adsorption isotherm and kinetic studies*. Journal of Hazardous Materials, 165(1-3), 100-110.https://doi.org/10.1016/j.jhazmat.2008.09.122
5. Nautiyal, P., Subramanian, KA., & Dastidar, MG., (2016) *Adsorptive removal of dye using biochar derived from residual algae after in-situ*

transesterification: alternate use of waste of biodiesel industry. Journal of environmental management, 182, 187-197. https://doi.org/10.1016/j.jenvman.2016.07.063

6. Tounsadi, H., Metarfi. Y., Barka, N., Taleb, M., & Rais, Z., (2020) *Removal of textile dyes by chemically treated sawdust of acacia: kinetic and equilibrium studies*. Journal of Chemistry, 2020, 1-12. https://doi.org/10.1155/2020/7234218
7. Mohamad, H. A. E. D., Amr, M. H. A., Bastawissi, A. A., Bastawissi, A. E., Panchal, H., & Sadasivuni, K. K. (2021). A portable active photovoltaic solar energy system in treating wastewaters by electrocoagulation. *Smart and Sustainable Manufacturing Systems, 5*(1), 120–128. https://doi.org/10.1520/SSMS20200076
8. Saravanan, R., Sathish, T., Sharma, K., Rao, A. V., Sathyamurthy, R., Panchal, H., & Abdul Zahra, M. M. (2023). Sustainable wastewater treatment by RO and hybrid organic polyamide membrane nanofiltration system for clean environment. *Chemosphere, 337*, 139336. https://doi.org/10.1016/j.chemosphere.2023.139336
9. Ozdemir, O., Turan, M., Turan, AZ., Faki, A., & Engin, AB., (2009) *Feasibility analysis of color removal from textile dyeing wastewater in a fixed-bed column system by surfactant-modified zeolite* (SMZ). Journal of Hazardous Materials, 166(2-3), 647-654. https://doi.org/10.1016/j.jhazmat.2008.11.123
10. Lin, JX., Zhan, SL., Fang, MH., Qian, XQ., & Yang, H., (2008) *Adsorption of basic dye from aqueous solution onto fly ash*. Journal of Environmental Management, 87:1, 193-200. https://doi.org/10.1016/j.jenvman.2007.01.001
11. Dutta, S., Gupta, B., Srivastava, SK., & Gupta, AK., (2021) *Recent advances on the removal of dyes from wastewater using various adsorbents: A critical review*. Materials Advances, 2(14), 4497-4531. DOI: 10.1039/D1MA00354B

12. Mohamad, H. A. E. D., Hemdan, M., Bastawissi, A. A. E., Bastawissi, A. E. M., Panchal, H., & Sadasivuni, K. K. (2021). Industrial wastewater treatment by electrocoagulation powered by a solar photovoltaic system. *Energy Sources, Part A: Recovery, Utilization, and Environmental Effects*, *47*(1), 9479–9489. https://doi.org/10.1080/15567036.2021.1950870
13. Kashefialasl, M., Khosravi, M., Marandi, R., & Seyyedi, K., (2006) *Treatment of dye solution containing colored index acid yellow 36 by electrocoagulation using iron electrodes*. International Journal of Environmental Science and Technology, 2(4), 365.
14. Xiao, H., Zhao, T., Li, CH., & Li, MY., (2017) *Eco-friendly approaches for dyeing multiple type of fabrics with cationic reactive dyes*. Journal of Cleaner Production, 165, 1499-1507. https://doi.org/10.1016/j.jclepro.2017.07.174
15. Barba, D., Beolchini, F., & Vegliò, F., (2001) *A simulation study on biosorption of heavy metals by confined biomass in UF/MF membrane reactors*. Hydrometallurgy, 59(1), 89-99. https://doi.org/10.1016/S0304-386X(00)00144-4
16. Ahluwalia, SS., & Goyal, D., (2007) *Microbial and plant derived biomass for removal of heavy metals from wastewater*. Bioresource technology, 98(12), 2243-2257. https://doi.org/10.1016/j.biortech.2005.12.006
17. Bulgariu, L., & Bulgariu, D., (2018) *Functionalized soy waste biomass-A novel environmental-friendly biosorbent for the removal of heavy metals from aqueous solution*. Journal of Cleaner Production, 197, 875-885. https://doi.org/10.1016/j.jclepro.2018.06.261
18. Oyebamiji, OO., Boeing, WJ., Holguin, FO., Ilori, O., & Amund, O., (2019) *Green microalgae cultured in textile wastewater for biomass generation and biodetoxification of heavy metals and chromogenic*

substances. Bioresource Technology Reports, 7, 100247. https://doi.org/10.1016/j.biteb.2019.100247

19. Camila dos Santos, CSL., Reis, MHM., Cardoso, VL., & de Resende, MM., (2019) *Electrodialysis for removal of chromium (VI) from effluent: Analysis of concentrated solution saturation*. Journal of Environmental Chemical Engineering, 7:5,103380. https://doi.org/10.1016/j.jece.2019.103380
20. Heiderscheidt, E., Postila, H., & Leiviskä, T., (2020) *Removal of metals from wastewaters by mineral and biomass-based sorbents applied in continuous-flow continuous stirred tank reactors followed by sedimentation*. Science of the Total Environment, 700, 135079. https://doi.org/10.1016/j.scitotenv.2019.135079
21. Shukrullah, S., Azam, M., Naz, MY., Toqeer, I., & Gungor, A., (2021) *Effective removal of chromium from wastewater with Zn doped Ni ferrite nanoparticles produced using co-precipitation method*. Materials Today: Proceedings, 47, S9-S12. https://doi.org/10.1016/j.matpr.2020.04.263
22. Wang, Z., Shen, Q., Xue, J., Guan, R., Li, Q., Liu, X., Jia, H., & Wu, Y., (2020) *3D hierarchically porous NiO/NF electrode for the removal of chromium (VI) from wastewater by electrocoagulation*. Chemical Engineering Journal, 402, 126151. https://doi.org/10.1016/j.cej.2020.126151
23. Park, HG., Kim, TW., Chae, MY., & Yoo, IK., (2007) *Activated carbon-containing alginate adsorbent for the simultaneous removal of heavy metals and toxic organics*. Process Biochemistry, 42:10, 1371-1377. https://doi.org/10.1016/j.procbio.2007.06.016
24. Meena, AK., Kadirvelu, K., Mishra, GK., Rajagopal, C., & Nagar, PN., (2008) *Adsorptive removal of heavy metals from aqueous solution by treated sawdust (Acacia Arabica)*. Journal of Hazardous Materials, 150:3, 604-611. https://doi.org/10.1016/j.jhazmat.2007.05.030

25. Gkika, DA., Mitropoulos, AC., & Kyzas, GZ., (2022) *Why reuse spent adsorbents? The latest challenges and limitations*. Science of the Total Environment, 822, 153612. https://doi.org/10.1016/j.scitotenv.2022.153612
26. Deng, J., Xiong, T., Xu, ., Li, M., Han, C., Gong, Y., Wang, H., & Wang, Y., (2015) *Inspired by bread leavening: one-pot synthesis of hierarchically porous carbon for supercapacitors*. Green Chemistry, 17(7), 4053-4060. https://doi.org/10.1039/C5GC00523J
27. Chen, W., Yang, H., Chen, Y., Chen, X., Fang, Y., & Chen, H., (2016) *Biomass pyrolysis for nitrogen-containing liquid chemicals and nitrogen-doped carbon materials*. Journal of analytical and applied pyrolysis, 120, 186-193.https://doi.org/10.1016/j.jaap.2016.05.004
28. Wang, J., Nie, P., Ding, B., Dong, S., Hao, X., Dou, H., & Zhang, X., (2017) *Biomass derived carbon for energy storage devices*. Journal of materials chemistry A, 5(6), 2411-2428. https://doi.org/10.1039/C6TA08742F
29. Chen, W., Gong, M., Li, K., Xia, M., Chen, Z., Xiao, H., Fang, Y., Chen, Y., Yang, H, & Chen, H., (2020) *Insight into KOH activation mechanism during biomass pyrolysis: Chemical reactions between O-containing groups and KOH*. Applied Energy, 278, 115730. https://doi.org/10.1016/j.apenergy.2020.115730
30. Liew, RK., Azwar, E., Yek, PNY., Lim, XY., Cheng, CK., Ng, JH., Jusoh, A., Lam, WH., Ibrahim, MD., Ma, NL., & Lam, SS., (2018) *Microwave pyrolysis with KOH/NaOH mixture activation: a new approach to produce micro-mesoporous activated carbon for textile dye adsorption*. Bioresource technology, 266, 1-10. https://doi.org/10.1016/j.biortech.2018.06.051
31. Azargohar, R., & Dalai, AK., (2008) *Steam and KOH activation of biochar: Experimental and modeling studies*. Microporous and

Mesoporous Materials, 110(2-3), 413-421. https://doi.org/10.1016/j.micromeso.2007.06.047

32. Veli, S., Arslan, A., Isgoren, M., Bingol, D., & Demiral, D., (2021) *Experimental design approach to COD and color removal of landfill leachate by the electrooxidation process*. Environmental Challenges, 5, 100369. https://doi.org/10.1016/j.envc.2021.100369
33. Yadav, AM., Nikkam, S., Gajbhiye, P., & Tyeb, MH., (2017) *Modeling and optimization of coal oil agglomeration using response surface methodology and artificial neural network approaches*. International Journal of Mineral Processing, 163:55-63. https://doi.org/10.1016/j.minpro.2017.04.009
34. Yadav, AM., Nikkam, S., Sundaram, A., Painkra, P., Raja, AK., & Arshad, Md., (2018) *Investigation and optimization of the recovery of coal fines using oil agglomeration process: Use of waste oils from different sectors*. Journal of Dispersion Science and Technology 39:5, 754-764. https://doi.org/10.1080/01932691.2017.1414610
35. Yadav, AM., Chaurasia, RC., Suresh, N., & Gajbhiye, P., (2018) *Application of artificial neural networks and response surface methodology approaches for the prediction of oil agglomeration process*. Fuel, 220:826-836. https://doi.org/10.1016/j.fuel.2018.02.040
36. Li, B., Huang, L., Lv, X., & Ren, Y., (2021) *Study on temperature variation and pore structure evolution within coal under the effect of liquid nitrogen mass transfer*. ACS Omega, 6:30, 19685-19694. https://doi.org/10.1021/acsomega.1c02331
37. Rangabhashiyam, S., & Balasubramanian, P., (2019) *The potential of lignocellulosic biomass precursors for biochar production: performance, mechanism and wastewater application-a review*. Industrial Crops and Products, 128, 405-423. DOI :10.1016/j.indcrop.2018.11.041
38. Ahuja, R., Kalia, A., Sikka, R., & Chaitra, P., (2022) *Nano Modifications of Biochar to Enhance Heavy Metal Adsorption from Wastewaters: A*

Review. ACS Omega, 7:50, 45825-45836. https://doi.org/10.1021/acsomega.2c05117

39. Ghanim, B., O'Dwyer, TF., Leahy, JJ., Willquist, K., Courtney, R., Pembroke, JT., & Murnane, JG., (2020) *Application of KOH modified seaweed hydrochar as a biosorbent of Vanadium from aqueous solution: Characterisations, mechanisms and regeneration capacity*. Journal of Environmental Chemical Engineering, 8:5, 104176. https://doi.org/10.1016/j.jece.2020.104176
40. Wang, S., Nam, H., & Nam, H., (2020) *Preparation of activated carbon from peanut shell with KOH activation and its application for H_2S adsorption in confined space*. Journal of Environmental Chemical Engineering, 8:2, 103683. https://doi.org/10.1016/j.jece.2020.103683
41. Surip, SN., Abdulhameed, AS., Garba, ZN., Syed-Hassan, SSA., Ismail, K., & Jawad, AH., (2020) *H_2SO_4-treated Malaysian low rank coal for methylene blue dye decolorization and cod reduction: optimization of adsorption and mechanism study*. Surfaces and Interfaces, 21, 100641. https://doi.org/10.1016/j.surfin.2020.100641
42. Devi, R., Singh, V., & Kumar, A., (2008) *COD and BOD reduction from coffee processing wastewater using Avacado peel carbon*. Bioresource technology, 99:6, 1853-1860. https://doi.org/10.1016/j.biortech.2007.03.039
43. Muthukumar, M., Sargunamani, D., Selvakumar, N., & Rao, JV., (2004) *Optimisation of ozone treatment for color and COD removal of acid dye effluent using central composite design experiment*. Dyes and Pigments, 63:2, 127-134.https://doi.org/10.1016/j.dyepig.2004.02.003
44. Perkins, WS., Law, SE., Smith, MC., Winger, PV., & Lasier, PJ., (2001) *Biological Treatability and Environmental Impact of Ozonation of Spent Reactive Dyebaths*. AATCC Review, 1(2).

45. Körbahti, Bahadır K., and Abdurrahman Tanyolaç. *"Electrochemical treatment of simulated textile wastewater with industrial components and Levafix Blue CA reactive dye: Optimization through response surface methodology."* Journal of hazardous Materials 151.2-3 (2008): 422-431. https://doi.org/10.1016/j.jhazmat.2007.06.010

46. Asgari, Ghorban., et al. *"Sonophotocatalytic treatment of AB113 dye and real textile wastewater using ZnO/persulfate: Modeling by response surface methodology and artificial neural network."* Environmental research 184 (2020): 109367. https://doi.org/10.1016/j.envres.2020.109367

47. Sharma, S., S. Kapoor., & R A, Christian., *"Effect of Fenton process on treatment of simulated textile wastewater: optimization using response surface methodology."* International Journal of Environmental Science and Technology 14 (2017): 1665-1678. https://doi.org/10.1007/s13762-017-1253-y

48. Bashir, Mohammed JK., et al. *"Wastewater treatment processes optimization using response surface methodology (RSM) compared with conventional methods: review and comparative study."* Middle-East J. Sci. Res 23.2 (2015): 244-252. https://doi.org/10.5829/idosi.mejsr.2015.23.02.52

49. Vyavahare, Govind D., et al. *"Response surface methodology optimization for sorption of malachite green dye on sugarcane bagasse biochar and evaluating the residual dye for phyto and cytogenotoxicity."* Chemosphere 194 (2018): 306-315. https://doi.org/10.1016/j.chemosphere.2017.11.180

50. Roy, Hridoy., et al. *"Synthesis, characterizations, and RSM analysis of Citrus macroptera peel derived biochar for textile dye*

treatment." South African Journal of Chemical Engineering 41 (2022): 129-139. https://doi.org/10.1016/j.sajce.2022.05.008

51. Perveen, Shazia., et al. "*Biochar-mediated zirconium ferrite nanocomposites for tartrazine dye removal from textile wastewater.*" Nanomaterials 12.16 (2022): 2828. https://doi.org/10.3390/nano12162828

52. Jagaba, Ahmad., & Hussaini., et al. "*Biochar-based geopolymer nanocomposite for COD and phenol removal from agro-industrial biorefinery wastewater: kinetic modelling, microbial community, and optimization by response surface methodology.*" Chemosphere 339 (2023): 139620. https://doi.org/10.1016/j.chemosphere.2023.139620

53. Fseha., Yohanna, Haile., Jamal, Shaheen. & Banu, Sizirici., "*Phenol contaminated municipal wastewater treatment using date palm frond biochar: Optimization using response surface methodology.*" Emerging Contaminants 9.1 (2023): 100202. https://doi.org/10.1016/j.emcon.2022.100202

54. Husien, Sh., et al. "*Review of activated carbon adsorbent material for textile dyes removal: Preparation, and modelling.*" Current Research in Green and Sustainable Chemistry (2022): 100325. https://doi.org/10.1016/j.crgsc.2022.100325

55. Laxmi, Deepak Bhatlu., M., et al. "*Preparation of Breadfruit Leaf Biochar for the Application of Congo Red Dye Removal from Aqueous Solution and Optimization of Factors by RSM-BBD.*" Adsorption Science & Technology 2023 (2023). https://doi.org/10.1155/2023/7369027

56. Saravanan, Praveen., et al. "*Evaluation of the adsorptive removal of cationic dyes by greening biochar derived from agricultural bio-waste*

of rice husk." Biomass Conversion and Biorefinery (2021): 1-14. https://doi.org/10.1007/s13399-021-01415-y

57. Kapoor, Riti Thapar., & Selvaraju ,Sivamani., *"Adsorptive Potential of Orange Peel Biochar for Removal of Basic Red 46 Dye and Phytotoxicity Analysis."* Chemical Engineering & Technology 46.4 (2023): 756-765. https://doi.org/10.1002/ceat.202200436

58. Abdrashitova, R. N., Bozhenkova, G. S., Ponomarev, A. A., Gilya-Zetinov, A. G., Markov, A. A., & Zavatsky, M. D. (2023). Synthesis of ZnO doped multi walled carbon nanotubes (MWNTs) for dyes degradation and water purification. Water Conservation & Management, 7(1), 01-05. https://doi.org/10.1016/j.envres.2025.121139

59. Da Silva Medeiros, D. C. C., Usman, M., Chelme-Ayala, P., & Gamal El-Din, M. (2025). Biochar-enhanced removal of naphthenic acids from oil sands process water: Influence of feedstock and chemical activation. Energy & Environmental Sustainability, 1(2), 100028. https://doi.org/10.1016/j.eesus.2025.100028

60. Gadekar, M. R., Akhtar, M., & Ahmaruzzaman, M. (2024). Optimization of atenolol removal using response surface methodology: Adsorption study on lignin-chitosan composite. Alexandria Engineering Journal, 92, 391-408. https://doi.org/10.1016/j.aej.2024.02.042

61. Iftikhar, A., Waris, A. A., Din, M. I., Saeed, M., Ambreen, J., Khalid, R., Asghar, M. A., & Shahid, M. (2024). Comparative study of RSM and ANN for the optimization of mechanical properties of polyester/Ag-ZnO nanocomposite. PLoS ONE, 19(1), e0294286. https://doi.org/10.1371/journal.pone.0294286

62. Kumar, A., Sharma, S. K., Pandey, L. M., & Chowdhury, S. (2025). Regeneration and reusability of biochar-based adsorbents for sustainable wastewater treatment: A critical review. Scientific Reports, 15, 11132. https://doi.org/10.1038/s41598-025-11132-5

63. Li, N., Zhu, F., Wang, Z., Wu, J., Gao, Y., Li, K., Zhang, L., Wang, H., & Wang, X. (2025). Harnessing corn straw biochar: A breakthrough in eco-friendly Cu(II) wastewater treatment. Waste Management, 197, 25-34. https://doi.org/10.1016/j.wasman.2025.02.027

64. Myers, R. H., Montgomery, D. C., & Anderson-Cook, C. M. (2016). Response surface methodology: process and product optimization using designed experiments (4th ed.). John Wiley & Sons.

65. Natarajan, E., Ramasamy, G., Abdullah, H., Sekar, S. M., & Abd Hamid, A. R. (2025). Emerging contaminants in water: An overview of causes, metrics, and treatment methods. In Sustainable structural materials: From fundamentals to manufacturing, properties and applications (pp. 241-255). CRC Press.

66. Nayak, A., Bhushan, B., & Kotnala, S. (2025). Regeneration strategies for spent biochar: A pathway toward circular economy in water treatment. Environmental Science and Pollution Research, 32(8), 11245-11267.

67. Rameshkumar, V., Kiruthika, E., Sowmya, N., & Kayalvizhi, R. (2023). Response surface methodology and artificial neural network for modeling and optimization of distillery spent wash treatment using Phormidium valderianum BDU 140441. Applied Water Science, 14(1), 6. https://doi.org/10.1007/s13201-023-02060-8

68. Tran, H. N., You, S. J., Hosseini-Bandegharaei, A., & Chao, H. P. (2025). Pitfalls of linear kinetic plots and significance of statistical analysis in

adsorption studies. South African Journal of Chemical Engineering, 49, 104-115. https://doi.org/10.1016/j.sajce.2025.07.004

69. Xu, Y., Fan, Z., Li, X., Yang, S., Wang, J., Zheng, A., Zhang, L., Chen, W., Wang, H., & Shu, R. (2024). Cooperative production of monophenolic chemicals and carbon adsorption materials from cascade pyrolysis of acid hydrolysis lignin. Bioresource Technology, 399, 130557. https://doi.org/10.1016/j.biortech.2024.130557

70. Yang, H., Wang, X., Wang, J., Liu, H., Jin, H., Zhang, J., & Ye, C. (2025). High-value utilization of agricultural waste: A study on the catalytic performance and deactivation characteristics of iron-nickel supported biochar-based catalysts in the catalytic cracking of toluene. Energy, 323, 135806. https://doi.org/10.1016/j.energy.2025.135806

71. Zhu, H., Ma, H., Xu, L., Yu, D., Zhong, S., Chen, Y., & Pu, S. (2025). The regulatory role of dissolved oxygen in N-doped biochar-driven nonradical oxidation. Chemical Engineering Journal, 520, 165915. https://doi.org/10.1016/j.cej.2025.165915

72. Mohamad, H. A. E. D., Amr, M. H. A., Bastawissi, A. A., Bastawissi, A. E., Panchal, H., & Sadasivuni, K. K. (2021). A portable active photovoltaic solar energy system in treating wastewaters by electrocoagulation. Smart and Sustainable Manufacturing Systems, 5(1), 120-128. https://doi.org/10.1520/SSMS20200046